Downscaling Coarse Resolution Satellite Passive Microwave SWE Estimates

by

Margot Flemming

A thesis
presented to the University of Waterloo
in fulfillment of the
thesis requirement for the degree of
Master of Science
in
Geography

Waterloo, Ontario, Canada, 2020

AUTHOR'S DECLARATION

I hereby declare that I am the sole author of this thesis. This is a true copy of the thesis, including any required final revisions, as accepted by my examiners.
I understand that my thesis may be made electronically available to the public.

Abstract

The spatio-temporal heterogeneity of seasonal snow and its impact on socio-economic and environmental functionality make accurate, real-time estimates of snow water equivalent (SWE) important for hydrological and climatological predictions. Passive microwave remote sensing offers a cost effective, temporally and spatially consistent approach to SWE monitoring at the global to regional scale. However, local scale estimates are subject to large errors given the coarse spatial resolution of passive microwave observations (25 x 25 km). Regression downscaling techniques can be implemented to increase the spatial resolution of gridded datasets with the use of related auxiliary datasets at a finer spatial resolution. These techniques have been successfully implemented to remote sensing datasets such as soil moisture estimates, however, limited work has applied such techniques to snow-related datasets. This thesis focuses on assessing the feasibility of using regression downscaling to increase the spatial resolution of the European Space Agency's (ESA) Globsnow SWE product in the Red River basin, an agriculturally important region of the northern United States that is widely recognized as a suitable location for passive microwave remote sensing research.

Multiple Linear (MLR), Random Forest (RFR) and Geographically Weighted (GWR) regression downscaling techniques were assessed in a closed loop experiment using Snow Data Assimilation System (SNODAS) SWE estimates at a 1 x 1 km spatial resolution. SNODAS SWE data for a 5-year period between 2013-2018 was aggregated to a 25 x 25 km spatial resolution to match Globsnow. The three regression techniques were applied using correlative datasets to downscale the aggregated SNODAS data back to the original 1 x 1 km spatial resolution. By comparing the downscaled SNODAS estimates to the original SNODAS data, it was found that RFR downscaling produced much less variation in results, and lower RMSE values throughout the study period than MLR and GWR downscaling, indicating it was the optimal downscaling method. RFR downscaling was then implemented on daily Globsnow SWE estimates for the same time period. The downscaled SWE results were evaluated using SNODAS SWE as well as *in situ* derived SWE estimates from weather stations within the study region. Spatial and temporal errors were assessed using both the SNODAS and *in situ* reference datasets and overall RMSEs of 21 mm and 37 mm were found, respectively. It was observed that the southern regions of the basin and seasons with higher downscaled SWE estimates were associated with higher errors with overestimation being the most common bias throughout the region.

A major contribution of this study is the illustration that RFR downscaling of Globsnow SWE estimates is a feasible approach to understanding the seasonal dynamics of SWE in the Red River basin. This is extremely beneficial for local communities within the basin for flood management and mitigation and water resource management.

Acknowledgements

First and foremost, I would like to thank my supervisor Dr. Richard Kelly for guiding me through my Master's degree and supporting me each step of the way. His continuous positive encouragement, motivation, understanding and extreme passion for research has allowed me to create my own academic path and I am extremely grateful to have him as a mentor. I look forward to continuing my academic journey with him as I pursue my PhD.

Many other members of the scientific community have been extremely helpful in guiding this research. Thank you to Dr. Nastaran Saberi for her guidance and advice during this process, without whom this work would not have been possible. During an ERASMUS research exchange at the Friedrich Shiller University Jena in Germany, I had the privilege to work with Dr. Alexander Brenning, who's knowledge and guidance of spatial statistics and R had a great influence in the direction this thesis took. A sincere thank you goes to Dr. Jonathan Price, who has helped provoke my interest in research and has inspired me to continue on this crazy journey we call academia. I would also like to express my appreciation to my thesis committee members, Dr. Colin Robertson and Dr. Chris Fletcher. I am additionally thankful to the Natural Sciences and Engineering Research Council (NSERC) of Canada for the financial support that assisted in the completion of this thesis.

Without the support of many friends and family, I would not be where I am today. Thank you to all of my lab mates; it has been an honour to work alongside all of you. The sheer talent and intelligence I have been surrounded by over the course of this work is incredible. A special thank you to Vicky Vanthof, whose ongoing support and friendship both in and out of the lab have been instrumental to my success.

I would like to express my gratitude to my parents who have always encouraged me to accept a challenge with open arms and have always supported my decisions. Along with the rest of my family, they have been vital in helping me stay sane and have fun while working on this thesis. Their continued support and encouragement while I pursue my academic goals pushes me to stay focused and it means the world to me to have them stand beside me every step of the way.

Last but definitely not least, a massive thank you goes to my partner Dylan, who has endured endless hours of listening to me bombard him with information on snow, statistics and my love for R. His unconditional support and encouragement through every step of the way has been more important than any words can express.

Preface

This thesis contains my manuscript article that is to be submitted for peer reviewed publication on the regression downscaling of Globsnow SWE from its 25 x 25 km grid to a 1 km spatial resolution grid in the Red River. The study describes the methodology and discusses the results of the experiment. The research presented here is the result of an ongoing collaborative partnership between me and my advisor Dr. Richard Kelly, as well as with Dr. Alex Brenning at Friedrich Schiller University (Jena), who provided insightful advice and guidance during the early stages of this endeavour. Editing, style and scientific comments have been provided by Dr. Richard Kelly throughout the development of this document, with my contributions to this work being the creation of the original draft along with subsequent edited versions.

Table of Contents

List of Figures

List of Tables

Chapter 1 Introduction

1.1 Context and Motivation

The spatial and temporal heterogeneity of seasonal snow in the northern hemisphere and its major socio-economic and environmental impacts make it an important component of the cryosphere. The spatial extent of seasonal snow in the northern hemisphere can vary from 3 million km^2 to 50 million km^2 during the winter season, with approximately 1.2 billion people relying on snowmelt for water resources (Marshall, 2011; Sturm, Goldstein, & Parr, 2017). The majority of mid- to high-latitude river basins in the northern hemisphere rely on snowmelt for stream regulation and the amount of water stored in a snowpack, measured as snow water equivalent (SWE), directly influences springtime streamflow (Barnett, Adam, & Lettenmaier, 2005). Climate change induced variances in temporal and spatial snow dynamics have been observed, with the highest rates of change occurring in northern snow dominated regions (Derksen & Brown, 2012; AMAP, 2017). Therefore, the ability to estimate real-time SWE is vital for hydrological and climatological predictions and forecasting spring time flooding in downstream communities.

The recognition of the importance of SWE in hydrological and climatological cycles has driven a wide array of research into methods for monitoring and understanding real-time SWE dynamics. *In situ* observations of SWE in northern latitudes are spatially and/or temporally sparse in coverage and are typically not representative of the surrounding landscapes (Derksen, Walker, & Goodison, 2005; Foster et al., 2005; Neumann, Derksen, Smith, & Goodison, 2006). The lack of acceptable *in situ* networks for observing SWE in the northern hemisphere has prompted the development of remote sensing (RS) methods for SWE monitoring (Dietz,

Kuenzer, Gessner, & Dech, 2012). The fact that microwave radiation penetrates a snowpack at specific wavelengths provides an opportunity for the retrieval of information regarding SWE to be inferred from both passive microwave (PM) and active microwave (AM) RS observations. AM and PM RS differ by the source of the observed microwave radiation, with advantages and disadvantages existing for both in monitoring SWE. Space-borne PM RS can provide daily SWE estimates in all weather conditions by observing the microwave radiation emitted from the Earth's surface at multiple frequencies (Chang, Foster, Hall, Rango, & Hartline, 1982; Clifford, 2010; Dietz et al., 2012). Satellite PM RS observations have been used for monitoring real-time SWE in the northern hemisphere since the 1970s, however, the coarse gridded spatial resolution of approximately 25 x 25 km and general uncertainty in the range of 30-60 mm of SWE (Hancock, Baxter, Evans, & Huntley, 2013; Liu, Li, Huang, & Tian, 2014; Luojus et al., 2014) associated with PM observations limits it to regional to global-scale applications. More recently, AM RS has been examined for SWE monitoring, given the finer spatial resolutions associated with its observations. Studies have reported the successful use of AM RS to estimate SWE from Ku and X band frequencies from ground-based radar systems (Yueh et al., 2009; King et al., 2012). However, the limited frequencies on space-borne SAR systems currently impedes its use for real-time monitoring of SWE in homogenous landscapes across the northern hemisphere. Therefore, PM RS remains the only feasible and accepted space-borne method for retrieving real-time estimates of SWE.

The coarse spatial resolution of satellite PM RS observations, however, remains problematic. To combat the issue of coarse spatial resolution limitations in other scientific applications, an interesting question is the extent to which downscaling methods that integrate

covariate data or statistical techniques to estimate a target variable at a finer spatial resolution than originally available can be applied. In RS fields, such as soil moisture estimation or climate prediction mapping, downscaling is a common practice, with many studies examining various methods and the uncertainties associated with them (e.g. Agam, Kustas, Anderson, Li, & Neale, 2007; Immerzeel, Droogers, de Jong, & Bierkens, 2009; Zaksek & Ostir, 2012). However, limited research has assessed these methods for downscaling satellite PM RS SWE estimates. Gao, Xie, Lu, Yao, & Liang, (2010) developed a SWE specific algorithm that successfully combines optical-based SCE and PM SWE data to estimate SWE in 2500 500 m x 500 m^2 subpixels within a 25 x 25 km PM grid cell. This study proves that downscaling satellite PM RS SWE observations is feasible, however, since this is a relatively new area of research for SWE monitoring, there is a lack of understanding in the multitude of available approaches and the feasibility of them. Therefore, this thesis examines the feasibility of implementing downscaling methods to satellite PM RS SWE estimates to produce local to regional SWE estimates.

1.2 Aims and Objectives

The overall aim of thesis is to explore how downscaling approaches could be implemented to coarse resolution gridded SWE estimates derived from PM RS observations, with an emphasis on regression downscaling. The implementation of downscaling techniques would expand the applicability of satellite PM RS observations for local to regional spatial scales. The specific objectives that will assist in achieving the overall aim are as follows:

i) explain the significance of monitoring SWE from space-borne observations and current methods of PM RS SWE monitoring;

ii) review the currently available downscaling methods and provide a detailed understanding of the regression downscaling technique;

iii) implement and evaluate regression downscaling to a 5-year period of coarse resolution PM RS-derived SWE estimates.

1.3 Thesis Structure

This thesis has been written following the manuscript style in which chapter 3 is a standalone paper. Chapter 2 provides background information on SWE and how it is measured through PM RS as well as downscaling approaches currently used in other RS fields, with a detailed explanation of regression downscaling. Chapter 3 is the standalone paper titled *Evaluation of regression downscaling of coarse resolution Globsnow SWE estimates in the Red River Basin.* Chapter 4 identifies challenges and limitations associated with regression downscaling, offers suggestions for future work in this field and provides a conclusion and outline of the scientific contribution made in this thesis.

Chapter 2 Background

2.1 The Importance of Snow Water Equivalent Monitoring

Seasonal snow has major socio-economic and environmental impacts regarding the hydrologic cycle, water resource management, the energy budget and the economy (Barnett et al., 2005). The spatial and temporal variability of snow cover extent and SWE impact the functionality of these systems and their sensitivity to climatic processes can have severe consequences in a warming climate.

Snow plays an important role in the hydrologic cycle by storing and releasing liquid water during the winter season. As precipitation falls as snow when air temperatures are below ~0° C, a snowpack can form on the Earth's surface. The water molecules present in the snowpack are stored as snow crystals until temperatures exceed 0° C when melt occurs (Daanen, Misra, & Thompson, 2011). Snow is a significant component of the hydrologic cycle that regulates the movement of water between the Earth and the atmosphere. A snowpack acts as a water reservoir, storing frozen water until spring, when the snow melt is released downstream. The amount of water stored in a winter snowpack is measured in millimetres (mm) as SWE, calculated by multiplying the depth of a snowpack by the density of the snowpack. Variations in SWE throughout the winter season directly affect the amount of springtime streamflow.

The majority of the river basins in the Northern Hemisphere are considered snowmelt dominated, implying that over 50% of the runoff contributing to streamflow originates from snowfall, with approximately one sixth of the world's population residing in those basins (Barnett et al., 2005). Over the past 60 years, snowmelt runoff has occurred earlier and more

frequently within the snow season in snow-dominated regions and it is predicted that the dominant winter precipitation type will increasingly transform from snow to rain in the coming years(Räisänen, 2008; Stewart, Cayan, & Dettinger, 2004). Barnett et al. (2005) examined the storage capacity of snow dominated basins globally to assess whether basins could handle an increase in seasonal streamflow that could occur with a climatic change in winter precipitation. It was concluded that only the only basins that could handle a shift in streamflow were the Colorado, the Churchill and the Grand Rivers in North America and the Angara River in Asia. Therefore, a climatic shift in the seasonal timing of SWE will directly affect the hydrological cycle, water resource management and economic practices in many river basins around the globe.

With more frequent melt events expected to occur during the winter season, the quantity of immobilized water within the hydrologic cycle at the end of the winter season will decrease, with an excess amount of water being released from the snowpack earlier in the season. This in-season increase in snowmelt will induce increases in other parts of the hydrologic cycle such as streamflow, groundwater discharge, and evapotranspiration. A decreased quantity of water being stored in the snowpack during the late winter months also severely impacts water resource management in downstream communities.

Approximately 1.2 billion people rely on snowmelt for potable water, hydropower generation and agriculture (Sturm et al., 2017). During the winter season in the Northern Hemisphere, between 2000 and 3000 km^3 of water is stored within the snowpack, much of which is released in the spring to downstream communities (Koskinen et al., 1999). Reservoir water used for human consumption is accumulated in the spring to meet water demands during the dry

season. In areas such as California, where snow cover is not prevalent, potable water originates from the mountain snowpack, making snowmelt important for water supply in more than just snow-dominated regions (Sturm et al., 2017). In snowmelt-dominated regions, groundwater and streamflow fed by snowmelt are necessary for human consumption and crop production (Barnett et al., 2005).

With a decrease in spring runoff due to less snow accumulation and earlier snowmelt, less water will be available for agriculture practices (Comis, 2011). Agriculture practices in the Canadian Prairies, for example, use a large amount of surface water for irrigation and are predicted to be at risk with a decline in spring and summer streamflow (Barnett et al., 2005).

Hydropower generation has become an alternative method of electricity production in mountainous areas to more environmentally destructive power generation methods such as nuclear or fossil fuel (Robinson, 1997). Hydropower generation accounted for 77% of global renewable energy generation and 18% of total energy consumption in 2012 (X. Zhang et al., 2018). With a predicted change in climate, hydropower generation will be directly affected by a change in precipitation and streamflow (Beheshti, Heidari, & Saghafian, 2019). Springtime snowmelt is relied upon by many communities for ensuring sufficient water is available for the dry season, either for human consumption, agricultural practices or hydropower generation.

Snow is also a crucial element of the Earth's energy budget by affecting the amount of both longwave and shortwave radiation being exchanged by the Earth and the atmosphere. A large proportion of the incoming shortwave radiation from solar illumination is reflected back into the atmosphere because of the high albedo of snow. Therefore, the amount of shortwave radiation being absorbed by the Earth's surface decreases when the surface is snow covered,

reducing surface warming by decreasing the net shortwave radiation (Cohen & Rind, 1991). Seasonal changes in snow also alter the net shortwave radiation. Fresh snow has the highest albedo, with proportions of reflected wavelengths greater than 0.90, whereas older snow that has undergone significant physical changes due to metamorphism has much lower albedos (T. Zhang, 2005). As the wavelength increases in the electromagnetic spectrum, the impacts of snow on the energy budget differ. Snow has one of the highest emissivities of longwave radiation than any other natural surface, implying that its absorptivity of longwave radiation is also high (T. Zhang, 2005). Atmospheric conditions determine the resulting temperature change of the snow surface. During cloud-free conditions, the amount of incoming longwave radiation is reduced, causing a greater amount of longwave radiation being emitted from a snowpack than absorbed, resulting in a cooling of the snow surface. However, under a cloudy sky with high amounts of moisture, the incoming longwave radiation is increased, resulting in a high amount being absorbed by the snow, and a warming of the snow surface (T. Zhang, 2005). With more variable snow cover being predicted, these areas of the energy budget will be affected. With less snow cover during the winter season, the amount of shortwave radiation being absorbed by the earth will increase, whereas the amount of longwave radiation being emitted will decrease. With more precipitation being predicted, specifically in the form of rain, moisture in the atmosphere will increase, resulting in an increase of the incoming longwave radiation (Barnett et al., 2005).

The impacts of snow on hydrological and climatological systems make it an important variable to monitor. The temporal and spatial variability of snow cover during the winter season has drastic effects on multi-scale water resource management. Therefore, quantifying SWE in

real-time at a local scale is beneficial to snow reliant communities in managing water supplies, as well as helping to better understand the climatological impacts at the basin scale.

2.2 Passive Microwave Remote Sensing for Snow Water Equivalent Estimation

The Earth naturally emits microwave radiation. Satellite PM sensors measure the quantity of the emitted microwaves from space as a brightness temperature (T_b) to obtain microwave thermal information about the landscape. When the Earth's surface is covered in snow, microwave radiation emitted from the underlying ground at certain frequencies are scattered away from the observed field of view, resulting in a reduction of the thermal signal reaching the PM sensor. As the snowpack increases in depth, the number of snow particles as well as the compaction of particles increase along the emission path, intensifying the amount of scattering, and decreasing the T_b further (Foster et al., 2005). This increased attenuation of the microwave signal with increased snow depth provides an opportunity to estimate depth or SWE from PM RS observations. The daily, all-weather capability and the long-term time series of spaceborne PM RS observations make it an advantageous method for monitoring snow.

Satellite PM RS has been used to estimate SWE since the 1970's beginning with the Electrically Scanned Microwave Radiometer (ESMR) sensor. However, spaceborne SWE emission research grew with the launch of the Scanning Multichannel Microwave Radiometer (SMMR) in 1978, the Special Sensor Microwave/Imager (SSM/I) in 1987 and the Advanced Microwave Scanning Radiometer – Earth Observing System (AMSR-E) in 2002. Algorithms that have been developed to estimate SWE from these sensors typically use the difference in T_b observed at two frequencies, usually 19 and 37 GHz (Chang, Foster, & Hall, 1987; Foster et al.,

2005; Kunzi & Patil, 1982 and others). The negligible scattering of microwaves within a snowpack at 19 GHz provides a background reference against which the SWE-dependent scattering at 37 GHz can be used to estimate SWE.

The original algorithms (e.g. Chang et al., 1987) were simplistic and easily reproducible. However, large uncertainties arose due to confounding effects of the presence of vegetation and the assumption that snow microstructure characteristics (stratigraphy, grain size, snow density) remain constant throughout a season. During the winter season, a snowpack undergoes metamorphism, and the snow crystals grow. As the snow crystals grow larger, microwave scattering increases, resulting in an overestimation in SWE (Foster et al., 1999).When vegetation is present, the emitted microwave signal reaching the sensor is both from the vegetation itself and the underlying snow-covered ground. This mixing effect results in a higher T_b recorded by the sensor and an underestimation of SWE (Cohen et al., 2015; Kruopis et al., 1999; Kurvonen & Hallikainen, 1997). Multiple studies have attempted to account for vegetation presence and snow crystal dynamics in the retrieval of SWE from spaceborne PM observations. (Foster et al., 2005) developed an algorithm using the same difference of frequencies but corrected for forest cover and snow crystal effects. Snow crystal information was derived from the work by Sturm, Holmgren, & Liston (1995) where North America was divided into different snow classes with varying snowpack characteristics and forest cover information was gained from the International Geo-sphere–Biosphere Program (IGBP) Land Cover Data Set (Loveland & Belward, 1997). Derksen (2008) also developed an algorithm to explore the uncertainty associated with forest cover by using the difference in T_b at the 18.7 and 10.7 GHz. It was found that in a boreal forest study site where deep snowpacks are common, this method proved better than using the typical

19 and 37 GHz difference. It has also been concluded that forest transmissivity is an influential parameter in the effect of forest cover on PM SWE retrievals (Kruopis et al., 1999; Langlois et al., 2011) prompting the development of SWE algorithms that include forest transmissivity. Li & Kelly (2017) examined the use of spaceborne Visible/ Infrared observations to estimate forest transmissivity and relate it to T_b in forested areas to assist in correcting PM SWE retrievals. As the effects of land cover and microstructure of snow on PM SWE retrievals become more understood, SWE retrieval algorithms are continuously updated to account for uncertainties found in current algorithms.

Multiple satellite PM SWE products have been developed to provide operational estimates of global SWE at monthly, weekly and daily temporal resolutions to varying levels of success. Monthly global SWE aggregates are available at NSIDC covering the time period of 1978 to 2011, using SMMR, SSM/I and AMSR-E PM observations in modified Chang algorithms. The Global Monthly EASE-Grid SWE Climatology Version 1 product used SMMR PM observations for the period between 1978-1987 and SSM/I PM observations for the period between 1987-2007 (Armstrong et al., 2005). The original Chang algorithm is first applied, using the difference in T_b at 18 (SMMR) or 19 (SSM/I) GHz and 37 GHz. Constant grain size and snow density estimates of 0.3 mm and 0.3 g/cm^3, respectively, are assumed and a forest fraction adjustment is applied for pixels determined as forest by a MODIS land cover dataset to estimate the final SWE value. The product is projected to a 25 km Equal-Area Scalable Earth (EASE) Grid.

The AMSR-E/Aqua Monthly L3 Global SWE EASE-grids Version 2 product estimated global monthly SWE projected to a 25 km EASE grid between the time period of June 2002 to

October 2011 through a modified Chang algorithm using AMSR-E PM observations at 18, 37 and 10.7 GHz (Kelly, Chang, Tsang, & Foster, 2003; Tedesco et al., 2004). Pixels classified as ocean, ice and mountains are first masked out using a MODIS land cover dataset. The original Chang algorithm using the difference between T_b at 18 GHz and 37 GHz is used, however, additional information from the T_b at 10.7 GHz is added to aid in detecting SWE in deep snowpacks and forested areas and a forest density variable is applied using a MODIS vegetation dataset. A forest fraction adjustment is then implemented using a MODIS land cover. Variable snow density values are determined by a global snow density dataset derived from in situ measurements from Brown & Braaten (1998) and Krenke (2004) to determine the final SWE estimation.

To capture the temporal variation in SWE within the monthly products, the Global EASE-grid 8 Day SSM/I SWE product is available at NSIDC for the time period between 2000 and 2008 (Brodzik et al., 2007). SWE is derived similarly to the Global Monthly EASE-Grid SWE Climatology Version 1, using the Chang algorithm with a forest fraction adjustment and constant grain size and snow density of 0.3 mm and 0.3 g/cm^3, respectively. The 8-day composite is created by using the maximum SWE in each pixel for every 8-day period.

Global daily SWE products available include AMSR-E daily L3 global SWE provided by the National Aeronautics and Space Administration (NASA)/ Japan Aerospace Exploration Agency (JAXA) and Globsnow SWE provided by the European Space Agency (ESA). The daily AMSR-E SWE product is produced using the same method as the monthly AMSR-E SWE product described above, using a modified Chang algorithm, and similarly, covers a time period between June 2002 and October 2011. The Globsnow SWE project, coordinated by the Finnish

Meteorological Institute (FMI), began in 2008 with the intention of creating a global long term SWE dataset to assist in climate research (Luojus et al., 2014). The first version of Globsnow (v1.0) was released in 2010, and the second (v2.0) was released in 2014, with significant improvements in data coverage and the removal inconsistencies due to sporadic weather station information (Luojus et al., 2014). The retrieval algorithm for producing both versions of Globsnow SWE estimates are similar, and only Globsnow v2.0 (referred to hereafter as Globsnow) will be discussed in detail. Globsnow provides daily estimates of SWE for the northern hemisphere projected to a 25 x 25 km EASE grid by combining PM RS observations with *in situ* measurements with weekly and monthly aggregated datasets also available. Synoptic weather station snow depth data from the European Centre for Medium-Range Weather Forecasts (ECMWF) is first interpolated to a 25 by 25 km gridded output of observed snow depth. Using an elevation dataset, pixels in the 25 km EASE-grid with an elevation standard deviation greater than 200m are classified as mountainous and are masked out, as well as the largest 1.5% of the snow depth data to deter from the addition of any false observations of deep snow. The observed snow depths are used as an input to the single layer Helsinki University of Technology (HUT) snow model, which simulates T_b values as a function of SWE, snow grain size and snow density (Pulliainen, 2006; Takala et al., 2011). Grain size is determined by fitting the simulated T_b values to the observed T_b values at weather station locations and optimizing grain size. Grain size estimates from the weather station locations are then interpolated using a kriging technique to obtain a spatially continuous grid of gran size estimates. A constant snow density value of 0.24 g/cm^3 is inputted into the HUT model. The HUT model is run using these inputs and a gridded output of simulated SWE. The simulated SWE values are then compared to

satellite PM SWE values using a cost function to determine the final estimate for SWE. The Globsnow project has been beneficial in producing daily estimates of SWE dating back to 1979. The long time series produced by Globsnow allows for long term snow research and trend analysis.

Numerous studies have evaluated the aforementioned products to determine where and when they perform best and whether they can be used for long term hemispheric SWE monitoring. Clifford (2010) examines the Global Monthly EASE-Grid SWE Climatology Version 1 product, finding lower seasonal SWE climatologies when compared to two SWE models, ERA40 and HadCM3, with the largest differences occurring in areas of high elevation and forest cover. Clifford (2010) suggests that satellite PM SWE products are best suited to areas such as the North American Great Plains, where most products have been calibrated to due to the higher density of in situ SWE measurements.

An extensive global comparison between monthly Globsnow, Global Monthly EASE-Grid SWE Climatology Version 1 and AMSR-E/Aqua Monthly L3 Global SWE EASE-grids Version 2 was completed by Liu et al. (2014). It was found that for SWE values between 30 mm and 200 mm, Globsnow performed better than the other two products with root mean squared errors (RMSEs) of 35.27 mm and 38.86 mm for the time periods between 1978-2002 and 2002-2010, respectively. In comparison, RMSE values of 62.23 mm and 54.40 mm were found for the Global Monthly EASE-Grid SWE Climatology Version 1 and AMSR-E/Aqua Monthly L3 Global SWE EASE-grids Version 2 products, respectively. Lower standard deviations and biases were also found for the Globsnow product. Liu et al. (2014) also concluded that the products available through NSIDC (AMSR-E, SSM/I) are more likely to underestimate SWE when

compared to Globsnow, and that Globsnow has an advantage to reduce uncertainties associated with snow metamorphism throughout a winter season due to the inclusion of varying snow grain size estimates over space and time. Globsnow was found to estimate SWE in deeper snowpacks more accurately than the NSIDC products with a SWE threshold of ~200 mm, whereas the Global Monthly EASE-Grid SWE Climatology Version 1 and AMSR-E/Aqua Monthly L3 Global SWE EASE-grids Version 2 products had a threshold of ~100 mm.

Another comparison of global SWE products was completed by Hancock et al. (2013) where AMSR-E/Aqua Monthly L3 Global SWE EASE-grids Version 2, Global EASE-grid 8 Day SSM/I SWE and Globsnow v1.0 where 1381 globally representative pixels were compared and validated using in situ SWE measurements during the time period of 2002 to 2008. It was concluded that the AMSR-E/Aqua Monthly L3 Global SWE EASE-grids Version 2 and Global EASE-grid 8 Day SSM/I SWE products are not as suitable for deeper snowpacks as Globsnow and tend to saturate around 150 mm, and that Globsnow is superior in capturing the peak accumulation date and melt onset date. Furthermore, Globsnow performed better in cold temperatures (<-35° C) when the AMSR-E/Aqua Monthly L3 Global SWE EASE-grids Version 2 and Global EASE-grid 8 Day SSM/I SWE products tend to overestimate SWE. Overall, it was concluded that all SWE products examined shows larger uncertainties during shoulder seasons due to sensitivities in PM RS observations to shallow snow packs and wet snow presence, however, it was concluded that throughout the winter seasons, Globsnow was the superior product at estimating SWE globally.

The superiority of Globsnow over other globally available SWE products found in studies such as Liu et al. (2014) and Hancock et al. (2013), as well as the long time-series associated

with Globsnow makes it the most reliable satellite global SWE product currently available. Therefore, Globsnow will be used as the primary satellite PM SWE product in this downscaling study within thesis. Globsnow facilitates synoptic scale climate applications and near-real time SWE monitoring with relatively low uncertainties. However, technical issues associated with PM sensors remain problematic. Passive microwave sensors are typically restricted to coarse spatial resolutions of approximately 25 x 25 km and are, therefore, currently ineffective for mountainous terrains as well as local to regional SWE monitoring applicability. Thus, methods for increasing the spatial resolution of gridded datasets through downscaling techniques should be considered for increasing the applicability of satellite PM RS observations.

2.3 Downscaling Coarse Resolution Gridded Spatial Data

Downscaling techniques can be applied to coarse resolution spatial data to gain information about a variable at a finer spatial resolution. Several areas of research including population mapping, weather forecasting, climate modelling and hydrology have successfully implemented downscaling methods on RS data, however, the implementation of these methods to PM RS SWE retrievals is un-tested. The availability of downscaling methods and their applicability to coarse resolution SWE estimates could facilitate more local-scale hydrological and water resource management applications. Several downscaling methods exist to solve this problem, including regression downscaling (RD), Area to Point Kriging (ATPK), Downscaling Cokriging (DSCK), Area to Point Regression Kriging (ATPRK) and dynamical downscaling. Each method has the same goal of increasing the spatial resolution of a gridded dataset, however, each with varying degrees of complexity, data requirement, and computing power. Given the lack of consideration and implementation of any of the aforementioned methods to coarse

resolution satellite SWE estimates, it is suggested that the simplest technique be applied as a starting point in this field of study. Therefore, the focus of this thesis will be RD to coarse resolution Globsnow SWE estimates and will be the only method described in full detail in the following sections.

2.3.1 Formulation of the Downscaling Problem

The goal of downscaling is to increase the spatial resolution of a gridded dataset. To formulate this problem mathematically, let $Z_s(v_{Si})$ represent the areal value of the continuous source variable Z_s with spatial support v_s at pixel i (i = 1…M, where M is the number of pixels in Z_s within the study domain D). The objective of downscaling methods is to estimate the same continuous variable at a finer spatial resolution for the same study domain D. Therefore, we let $\hat{Z}_s(v_{Tj})$ represent the predicted areal value of the source variable Z_s at the target spatial resolution v_T at pixel j(j = 1…N, where N is the number of pixels in the target grid of $\hat{Z}_s$ and M<N within the study doman D). The problem of downscaling RS data is therefore, how to transform $Z_s(v_S)$ to $\hat{Z}_s(v_T)$. This problem can be addressed through RD, which uses regression techniques and covariates to determine $\hat{Z}_s(v_T)$.

2.3.2 Regression Downscaling Approaches

RD predicts the source variable at a specific location x, written as $\hat{Z}_s(x)$ by the formulation of a regression equation. The theory behind RD is that a regression equation describing the source variable $Z_s(v_S)$ is formulated at the source variable spatial resolution (v_S) using related covariable(s) available at a fine resolution. The regression equation formulated at

the source spatial resolution is then applied to the original covariable(s) at the target spatial resolution (v_T). This concept is explained through the flow diagram in **Figure 2.1**.

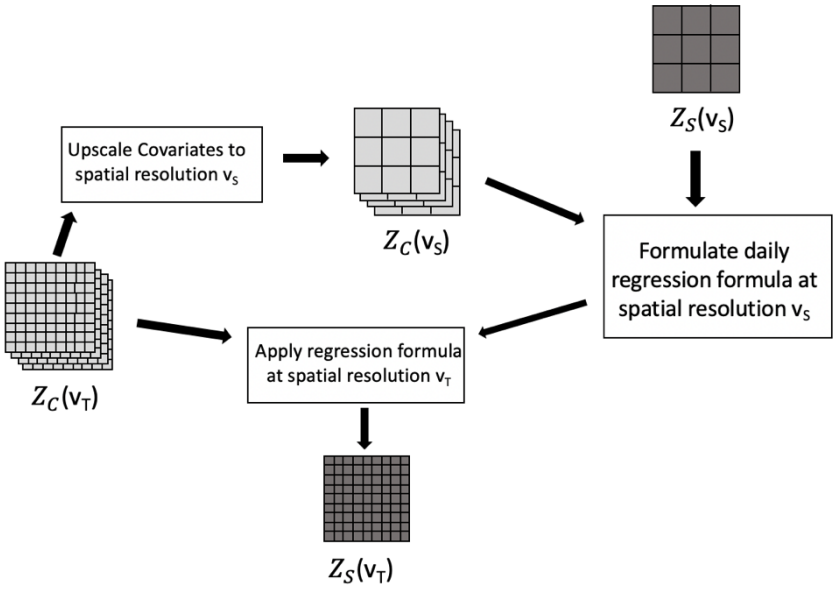

Figure 2.1: Schematic of Regression Downscaling Workflow

To further understand RD, a basic example can be explained using the simple linear regression (SLR) approach. For SLR RD, one covariable related to the source variable, written as $Z_c(v_T)$, where the target spatial resolution (v_T) is incorporated into the following regression equation:

$$\hat{Z}_s(x) = a_1 Z_c(x) + b_1 \quad (2.1)$$

where a_1 and b_1 are the SLR coefficients. The SLR coefficients are estimated at the source variable spatial resolution (v_S) by aggregating (or upscaling) the covariable to the same resolution. The regression coefficients are commonly estimated based on the least squares principals through a set of two normal equations. A linear line of best fit is generated to ensure the sum of the squared residuals for all M observations is minimized (Ryan, 2009). The SLR

model is generated at the source resolution and then applied at the target resolution (v_T) to estimate $Z_s(v_T)$.

Changing the regression technique used can increase the accuracy of the downscaled results by representing the true relationship between the source variable and the covariable(s). Common regression techniques used in RD are SLR, multiple linear regression (MLR), geographically weighted regression (GWR) and random forest regression (RFR). These regression methods are simple to implement and reproduce and will, therefore, be the methods adopted in this thesis.

MLR is the multivariate version of SLR, incorporating multiple covariates with the target spatial resolution (v_T) into equation 2.1 to become the following equation:

$$\hat{Z}_s(x) = \sum_{i=1}^{K} a_i Z_{ci}(x) + b_1 + \varepsilon_x \quad (2.2)$$

where K is the number of covariates used to downscale the source variable. In an MLR downscaling approach, K+1 coefficients are formulated at the source spatial resolution and the regression formula is then implemented at the target variable to estimate $\hat{Z}_s(v_T)$. Similarly to the formulation of the SLR model, the sum of squared residuals of the observations in the MLR model are minimized in accordance to the least squares principals, however, a set of K+1 normal equations are needed to estimate the coefficients in an MLR model, making it more computationally expensive (Bottenberg & Ward, 1963). Both MLR and SLR techniques make certain assumptions regarding the linearity, independence, normality, and equality of variance of the data (Ryan, 2009). Therefore, in cases where these assumptions are not valid, SLR and MLR may not be a viable technique to be applied. When these assumptions are met, however, MLR can be advantageous over SLR given that multiple covariates which can describe the source

variable can be incorporated, reaching a better representation of the true distribution of the source variable.

Both SLR and MLR are global regression approaches, where one regression model is formulated for the entire study domain, assuming the relationship(s) between the source variable and the covariate(s) do not change over space. GWR uses the same framework as SLR and MLR, however, is a weighted, localized variation where the linear regression formulas seen in equations 2.1 or 2.2 vary over space, accounting for the non-stationarity of most geographical datasets (Wheeler & Páez, 2010). Conversely to the SLR and MLR models, a new regression formula with a varying set of coefficients is generated at each source resolution grid cell i (i = 1…M). A window, or bandwidth size surrounding the regression point i is defined, which can either be static in varying across the study domain, and the observations within the window are used to generate a linear regression formula for the regression point. The advantage of using GWR over a simple moving window regression is the weighted linear regression model formulated within each window, giving a higher weight to observations closer in distance to the regression point (**Figure 2.2**). Therefore, a set of weights w_{ij} is defined for every *j* point within the window of the regression point *i* based on the distance d_{ij} between the points *i* and *j*. GWR is advantageous in capturing the spatially varying relationship between the source variable and the covariates if they exist and is a common regression technique for analyzing spatial datasets.

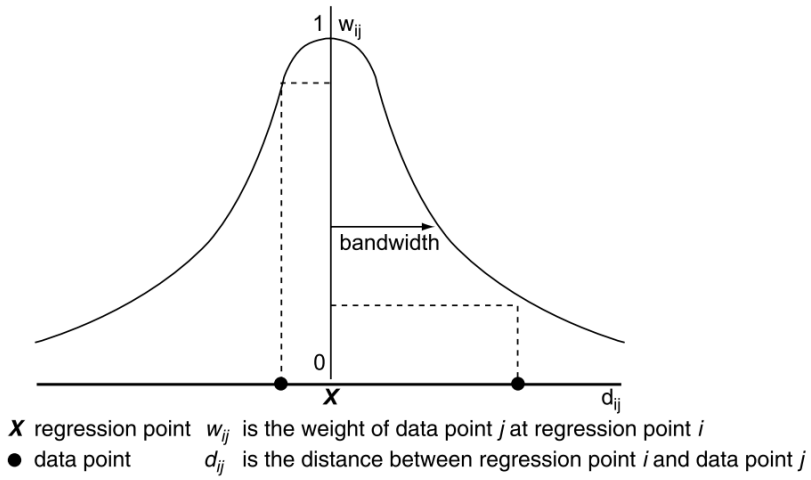

Figure 2.2: Visual representation of formulation of weights within a neighbourhood in Geographically Weighted Regression (Fotheringham, Brunsdon, & Charlton, 2002)

SLR, MLR and GWR are linear regression approaches, assuming that the relationship between the source variable and the covariate(s) can be represented by a linear manner. RFR is an ensemble, non-linear regression bagging approach where a set of non-correlated decision trees are constructed and averaged to find the best regression model. A decision tree predicts the source variable by using a random subset of the source variable observations and the covariate observations. As an ensemble approach, multiple decision trees are incorporated, creating a forest of decision trees, each producing a prediction of the source variable. A major differentiating feature between RFR algorithm and regular bagging approaches is the randomized subset of covariates used in each node split of the decision tree. Typically for each split, only a third of the covaraites are used in the randomized training sample, creating much more independence between trees and reducing variance (Breiman, 2001). The predictions made from each tree within the forest are then averaged to produce the final model output. The ensemble

characteristic of RFR is beneficial in minimizing uncertainty associated with predictions made from one decision tree and thus has been a commonly used regression technique (Brieman, 2001). RFR is able to capture relationships between the source variable and the covariate(s) that cannot be represented linearly. It is also beneficial in minimizing overfitting and is extremely user friendly with minimal parameters to be set by the user (Liaw & Wiener, 2002).

The aforementioned RD approaches have been successfully implemented to downscale satellite-derived land surface temperatures (LST), precipitation and soil moisture datasets. The TsHARP algorithm (originally called disTRAD), developed by Kustas, Norman, Anderson, & French (2003) uses least square regression to downscale 1 km LST observations by exploiting the relationship between LST and normalized difference vegetation index (NDVI). The TsHARP method was used extensively for the next decade and a half (e.g. Agam et al., 2007; Anderson et al., 2004) until studies examined the use of different regression techniques. Hutengs & Vohland (2016) compared the TsHARP algorithm with RFR RD and found and improvement of 19%. Duan & Li (2016) examined the applicability GWR RD for estimating LST at a finer spatial resolution, and also found an improvement when compared to the TsHARP method. RD has also been used to downscale coarser source resolution datasets such as Tropical Rainfall Measuring Mission (TRMM) precipitation and PM soil moisture estimates with success. Chen, Zhao, Duan, & Qin (2015) compared SLR, MLR and GWR RD approaches to increase the spatial resolution of the TRMM precipitation product from 0.25° to 1 km^2, finding that GWR outperformed the other two regression techniques, followed by MLR and lastly SLR. Yu, Di, & Yang (2008) examined MLR and GWR based downscaling methods to increase the spatial resolution of PM soil moisture estimates from 25 km to 1 km. It was concluded that the GWR based methods

performed better than the MLR methods, and that using an adaptive bandwidth in the GWR RD method was more accurate than using a fixed bandwidth.

RD is an easily reproducible and versatile approach to increasing the spatial resolution of gridded datasets and is a suitable technique to be applied initially given its simplicity. Given that RD has not been applied to coarse resolution SWE estimates, this method will be tested in this study to assess its feasibility and accuracy.

2.4 Implementation of Regression Downscaling on Coarse Resolution SWE Estimates

RD is a suitable approach to be tested on coarse resolution satellite PM SWE estimates given the different techniques available to be implemented to best describe the relationship between SWE and related covariables. Therefore, this thesis examines the feasibility, reliability and accuracy of implementing multiple RD methods to coarse resolution satellite PM SWE estimates at the basin scale. Through the comparison studies of different SWE products discussed in Section 2.2 (Hancock et al., 2013; Liu et al., 2014), it is acknowledged that while Globsnow SWE is the most reliable long-term dataset currently available to estimate SWE at the daily, global scale, there remain uncertainties in its estimation power. Nevertheless, Globsnow is the dataset of interest in this study.

As an initial implementation of RD to coarse resolution Globsnow SWE estimates, a study site that reduces landscape-derived uncertainties is desired. Extensive research on satellite PM SWE estimates has been performed and it is well known that non-complex landscapes are better suited for such estimates than others. Two major landscape-derived sources of uncertainties for PM SWE estimation are forest cover and topographical relief.

It is recognized that forested areas can severely increase the uncertainty associated with PM SWE estimates (Foster et al., 2005). The observed T_b in a densely forested areas is made up of the microwaves emitted from the snowpack, but also the microwaves emitted from the forest canopy, resulting in an underestimation up to 50% (Armstrong & Brodzik, 2001; Brown, Brasnett, & Robinson, 2003; Chang, Foster, & Hall, 1996). Satellite PM SWE estimates have been shown to perform better in open areas with low forest cover when compared to in situ measurements (Derksen, Walker, & Goodison, 2003). Furthermore, forest cover is known to also affect the retrievals in the visible part of the electromagnetic spectrum as well, affecting datasets such as MODIS snow cover, which could be a practical covariate in the RD approach.

In many satellite PM SWE products, including Globsnow, mountainous areas with high topographical relief are removed due to mixed pixel effects increasing the uncertainty of the SWE estimates (Kelly et al., 2003; Luojus et al., 2014). Problems associated with a varying microwave emission along a mountain range and the coarse resolution of satellite PM observations have shown estimates in these areas to be unreliable (Foster et al., 2005; Mätzler & Standley, 2000). Commonly, an elevation dataset is used to classify coarse pixels as mountainous by examining the difference in elevation between adjacent pixels (e.g. Kelly et al., 2003) or by examining the standard deviation of elevation within a coarse resolution pixel (e.g. Luojus et al., 2014).

The increased uncertainty of PM SWE estimates such as Globsnow in complex terrains such as forested and/or mountainous regions is reason to test RD in a study site that is located in an area with low forest cover and low topographical relief. The Red River of the North (Red River) and Devils Lake basins make up a cropland dominated region of the United States

dividing northwestern Minnesota and eastern North Dakota and has been chosen as a test site for RD in this study (**Figure 2.2**). Devils Lake basin is 9868 km^2 closed endorheic subbasin within the Red River basin in which water is contained within and does not contribute to the Red River unless severe flooding occurs (Todhunter, 2016). Home to approximately 22 000 residents, Devils Lake basin is comprised of Devils Lake and Stump Lake, however increasing water levels over the past decades have merged the two lakes into one water body since 2007, and hereafter will be referred to solely as Devils Lake (Vecchia, 2008). Flooding in Devils Lake basin is a severe problem to the residents, with over $1 billion USD of flood related damages between 1992 to 2011 alone (Zheng, Barta, & Zhang, 2014). A major problem with flooding in Devils Lake basin is the quality of the water from Devils Lake. Terminal lakes are typically high in salinity, and Devils Lake particularly is also extremely high in sulfate, making a release of water from Devils Lake basin to surrounding water bodies within the Red River basin an ongoing

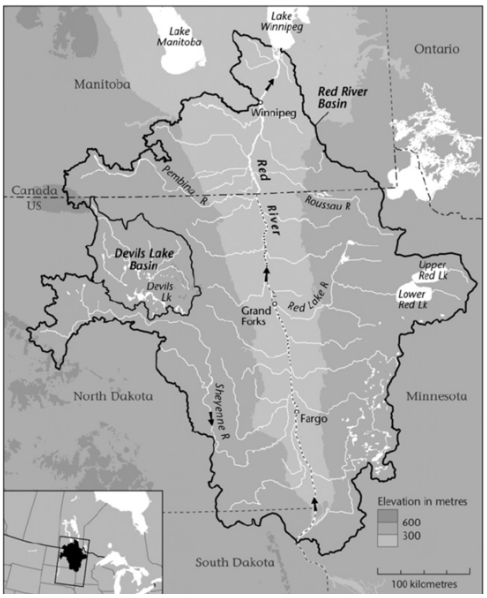

Figure 2.3: The Red River and Devils Lake basins

controversial issue (Zheng et al., 2014). Few natural overspills from Devils Lake basin to the Red River basin have occurred in the past, however, water levels in Devils Lake have increased 9.13 m between 1992 and 2013, and a further increase of 1.65 m would connect Devils Lake to Sheyenne River, a tributary of the Red River (Todhunter, 2016). Understanding the direct influence of changing water levels from spring snowmelt within Devils Lake basin is necessary for the communities within the basin, but also the communities within the Red River basin, which will be directly affected from an overspill from Devils Lake basin.

The Red River basin, the larger basin surrounding Devils Lake basin, is also an extremely flood prone regions of high agricultural importance. The headwaters of the Red River are located at the merge convergence of the Bois de Sioux and Otter Tail Rivers, located between Minnesota and North Dakota. The River flows northward into Canada, draining into Lake Winnipeg before meandering for 885 km within a relatively flat and cropland dominated floodplain in the Red River valley (Wang & Russell, 2016). The northward flow of the river makes the region more susceptible to springtime flooding since the southern portions of the river of melt earlier than the northern parts, causing a blockage for upstream flow (Schwert, 2003). The flat topography within the Red River basin and the low permeability of the soil is also flood inducing and has resulted in floodplains reaching widths of 40 km (Burn, 1999; Wang & Russell, 2016). Major floods over the past few decades have occurred in 1997, 2006, 2009 and 2011, each causing substantial economic, agricultural and personal damages. Furthermore, research from Hirsch & Ryberg (2012) and Rice, Emanuel, Vose, & Nelson (2015) indicates that flood frequency in this region is expected to rise in a changing climate.

Although the Red River basin and Devils Lake basin differ hydrologically, the geographical similarities and shared need for flood management suggest that both areas can significantly benefit from a better understanding of seasonal SWE dynamics on a finer spatial resolution than currently available. Therefore, this study examines the feasibility of RD methods in both basins and combines them into one study domain.

To downscale satellite PM SWE estimates using RD, related covariables available at the target spatial resolution or finer are required to generate the regression models. In this study snow cover fraction, normalized difference vegetation index (NDVI), elevation and land surface temperature (LST) were the four covariates used. These covariates are all satellite derived variables which are freely available at fine resolutions and can help describe the variability of SWE. Snow cover fraction derived from a binary snow cover extent dataset at a fine spatial resolution can give indication to how much snow is present in a course spatial resolution pixel. It has been documented that SWE is highly influenced by microtopography and vegetation giving reason for NDVI and elevation covariates to help describe SWE variability within the study region (Derksen et al., 2005). LST has been found to be negatively correlated to SWE, especially in the shoulder seasons (Matsui, Lakshmi, & Small, 2003), and can therefore, be an indicator of SWE variability when snow is starting to accumulate or melt.

The following chapter is a standalone paper that outlines the datasets and methodology used in the implementation of RD to Globsnow SWE estimates in the Red River basin and discusses the results found through an experimentation study.

Chapter 3 Evaluation of Regression Downscaling of Coarse Resolution Globsnow SWE Estimates in the Red River Basin

3.1 Introduction

The variation in seasonal snow accumulation both spatially and temporally during the winter season has major socio-economic and environmental impacts and current real-time monitoring techniques are inefficient at capturing the spatio-temporal variation for local applicability. Accurate estimation of snow water mass stored in a winter snowpack, expressed as snow water equivalent (SWE), is vital for hydroclimatology predictions and for managing water supplies in downstream communities. In northern latitudes, *in situ* SWE measurements are spatially and/or temporally sparse and permanent monitoring station locations are not typically representative of the varying characteristics of snow in space and time (Derksen et al., 2005; Neumann et al., 2006). The lack of reliable information available from *in situ* measurements has prompted the development of remote sensing methods for snow monitoring since the 1960s (Dietz et al., 2012).

Satellite remote sensing provides a cost-efficient technique to monitoring temporally and spatially consistent seasonal SWE. Microwave sensors that observe snow at synoptic scales can infer information regarding snow depth (SD) and SWE (Hall, Kelly, Foster, & Chang, 2005). Passive microwave (PM) sensors observe the emitted radiation from the Earth's surface which is typically attenuated by dry snow, measured as temperature brightness (T_b). SWE can be estimated by the T_b difference between 36GHz and 19GHz, or δT_b (Chang et al., 1987; Foster et al., 2005). In thin snowpacks, δT_b is zero resulting in no detection of snow (Clifford, 2010). An

upper SD limit of ~1m also exists due to loss of sensitivity of the 36GHz channel at thicker depths (Foster et al., 2005). In addition, when water is present in a snowpack, or the soil below a snowpack, the emissivity increases in the 36GHz channel and δT_b is close to or less than zero even if SD/SWE is greater than 0 (Clifford, 2010; Kelly et al., 2003). Therefore, PM remote sensing can only be used to estimate SD/SWE of dry, developed snowpacks with depths less than ~1 m.

Despite these limitations, PM remote sensing has been acknowledged as a relatively consistent and robust measurement tool for global SD and SWE estimates. Several coarse resolution products have been developed from PM remote sensing observations to estimate SWE globally. Globsnow SWE v2.0, referred to in this study as Globsnow, is a satellite-based product from the European Space Agency (ESA) (Luojus et al., 2014; Mudryk, Derksen, Kushner, & Brown, 2015; Pulliainen, 2006; Takala et al., 2011) that covers a 40-year time series of gridded daily SD and SWE estimates in the Northern Hemisphere at 25 x 25 km spatial resolution. Although studies have assessed Globsnow's accuracy to monitor SWE at regional to global scales (e.g. Larue et al., 2017; Liu et al., 2014; Luojus et al., 2014; Snauffer, Hsieh, & Cannon, 2016) it is unclear whether coarse spatial resolution PM SWE estimates (25 x 25 km grid cells) can be used for finer local/regional spatial scale purposes. Fine scale resolution SD/SWE products such as the Snow Data Assimilation System (SNODAS), a daily assimilated SWE product for the United States with a 1 x 1 km spatial resolution, are beneficial in understanding the temporal and spatial dynamics of SWE, however, typically rely heavily on *in situ* data and no global product is available. Consequently, a knowledge gap exists regarding spatially and

temporally consistent monitoring of fine scale SD and SWE with a large spatial coverage for local to regional hydrological, climatological, social and economic applications.

Regression downscaling (RD) is a statistical technique that can be applied to coarse resolution gridded data that facilitates information to be modelled at a finer spatial resolution. RD uses related covariates available at a fine resolution to formulate a regression model that is used to downscale the course resolution variable to the same resolution as the covariates. Common RD approaches, including multiple linear regression (MLR), geographically weighted regression (GWR) and random forest regression (RFR) have been successfully employed for weather forecasting, climate modelling, soil moisture estimation and hydrological applications (e.g. Agam et al., 2007; Immerzeel, Rutten, & Droogers, 2009; Zaksek & Ostir, 2012), however, limited work has involved applying such methods on PM remote sensing derived SD or SWE retrievals. Therefore, this study focuses on the implementation of common RD approaches on coarse resolution SWE estimates to assess the ability of downscaling available SWE products such as Globsnow.

The overall aim of this study is to determine the feasibility to downscale coarse resolution SWE estimates to a 1 x 1 km spatial resolution without losing the reliability of the estimates. The specific objectives of this study are as follows:

i. Determine the optimal RD method from the following three regression techniques: Multiple Linear Regression (MLR), Random Forest Regression (RFR) and Geographically Weighted Regression (GWR). These are selected because they represent linear and non-linear approaches as well as covering both local and global regression techniques;

ii. Apply the optimal RD method to five full winter seasons of coarse resolution Globsnow SWE estimates;

iii. Evaluate the performance of the optimal RD method by examining the spatial and temporal distribution of error of the downscaled SWE estimates.

3.2 Study Area

This study is conducted in the Red River and Devils Lake basins in the northern United States (**Figure 3.1**). Devils Lake basin is a closed, flood-prone basin within the Red River basin where water enters mostly by precipitation and departs through evaporation, typically not adding to the flow of the Red River. However, the probability of a natural overflow into the Sheyenne River, a tributary of the Red River, is between 8 to 20 % (Brandson & Hearne, 2013). Flooding within Devils Lake basin is common and problematic to the 22 000 people residing within the ~1000 km^2 area. Although the two basins are geographically separate, in this study they will be considered together and referred to as the Red River basin, since fine scale SWE estimation is equally important in both areas for flood management and mitigation.

The Red River basin is located in eastern North Dakota and northeastern Minnesota, with the Red River flowing north from the Bois de Sioux River in Wahpeton, North Dakota and draining into Lake Winnipeg in Winnipeg, Canada. Although, the basin extends across the US-Canada border, only the portion within the US is examined in this study, due to in situ data availability.

The topography of the Red River basin is predominately a flat, glacial lake plain created by Glacial Lake Agassiz (Emerson, Vecchia, & Dahi, 2005). The Red River basin is an important hydrological and agricultural region of the United States with approximately 85% of

the 100 000 km^2 region covered by cropland irrigated using water from the Red River (Stoner, Lorenz, Wiche, & Goldstein, 1993). The major cities in the basin (Grand Forks, Fargo, Moorhead) rely directly on the Red River for water resources, whereas the smaller towns located inland from the river rely heavily on groundwater within the basin and tributaries of the Red River (Stoner et al., 1993).

The lack of topographic relief in the Red River basin makes it extremely susceptible to flooding since overbank flow events are able to reach a much larger area than most floodplains (Rannie, 2016). Springtime flooding influenced by the seasonal changes in snow cover and SWE in the Red River basin is a persistent environmental and economic issue with major flood events occurring in 1826, 1852, 1861, 1950, 1979, 1996, 1997, 2018, as well as many minor events within the past 200 years. The 1997 flood in the Red River basin, also known as the "Flood of the Century", saw flood waters extending 40 km in width and monetary damages of 500 million USD within the basin (Burn, 1999; Farlinger et al., 1998). The accurate monitoring of SWE at the basin scale is critical for communities in the Red River basin, where seasonal snowmelt is a large contributor to springtime flooding to help in understanding the spatio-temporal dynamics of snow and how it affects multi-scale hydrological and climatological cycles (Barnett et al., 2005; Gong, 2004).

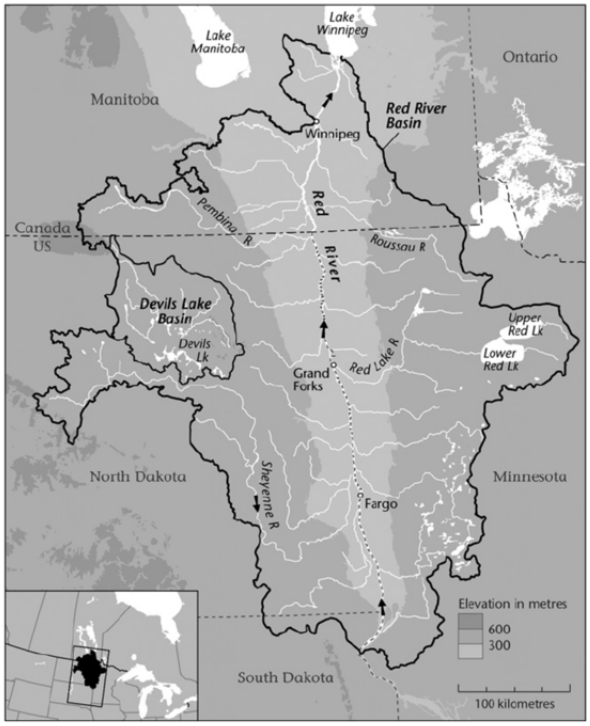

Source: Original Map by Eric Leinberger, University of British Columbia.

Figure 3.1: The Red River Basin

3.3 Methods and Data

3.3.1 Formulation of Regression Downscaling

Downscaling can be defined as the increase of spatial resolution, or the decrease in pixel size when regarding gridded datasets such as the Globsnow SWE product. The generic formulation of this problem can be represented mathematically where $Z_{ij}(v_i)$ represents the areal value of the input variable Z_i with spatial resolution v_i at pixel j (j = 1…M), where M is the number of pixels in Z_i within the study domain D. The objective of downscaling is to predict the same continuous variable as the original input data, Z_i, at a finer spatial resolution for the same study domain. Therefore, we let $\hat{Z}_{ij}(v_T)$ represent the predicted areal value of the input variable Z_i

at the target spatial resolution v_T at pixel j (j = 1…N, where N is the number of pixels in the target grid and M<N) within D. The problem of downscaling remote sensing data is therefore, how to transform $Z_i(v_i)$ to $\hat{Z}_i(v_T)$.

This study utilizes a regression downscaling method to solve this problem. Regression downscaling allows for the input variable, to be predicted at a specific location, x, denoted by $\hat{Z}_i(x)$ through the formulation of a regression equation. For a simple linear regression approach, a covariable related to Z_i, $Z_c(v_T)$, with the target spatial resolution v_T, is incorporated into the following regression equation:

$$\hat{Z}_i(x) = a_1 Z_c(x) + b_1$$

Where a_1 and b_1 are the regression coefficients. The regression coefficients are estimated at the spatial resolution of the input variable (v_T) by aggregating (upscaling) the covariate to the input variable spatial resolution to obtain $Z_c(v_T)$,. The regression formula obtained at the spatial resolution v_i is then applied at the target spatial resolution (v_T) (Hutengs & Vohland, 2016). **Figure 3.2** displays a visual schematic of how regression downscaling is applied. Multiple regression techniques can be applied in regression downscaling with a varying number of covariables. In this study, multiple linear regression (MLR), random forest regression (RFR) and geographically weighted regression (GWR) approaches were applied and four covariates were used to predict SWE at a 1 x 1 km spatial resolution for five winter seasons between October 2013 and April 2018.

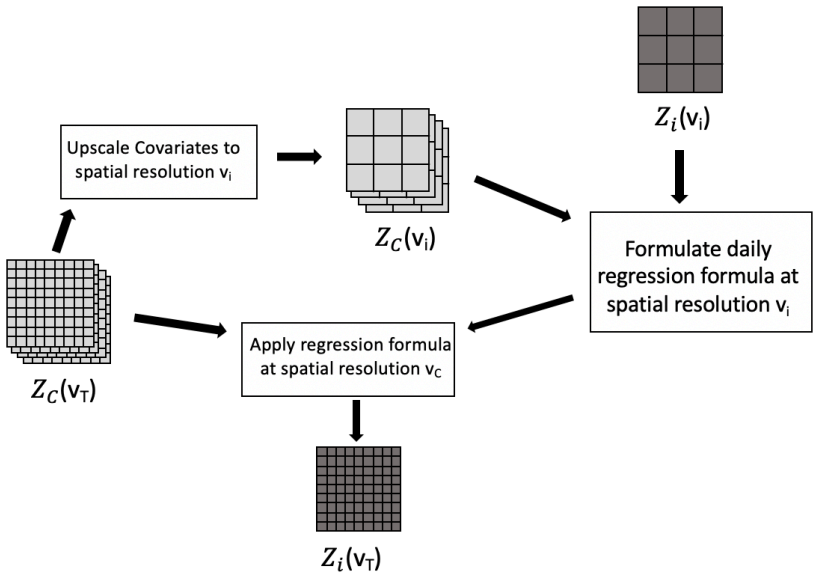

Figure 3.2: Workflow presenting steps implemented for regression downscaling

3.3.2 Datasets

3.3.2.1 SNODAS SWE Data

SNODAS was developed by the National Weather Service's National Operational Hydrological Remote Sensing Center (NOHRSC) in 2003 and is freely available through the National Snow and Ice Data Centre (NSIDC). SNODAS provides daily fine scale SWE estimates for the United States and the southern portion of Canada by assimilating model, satellite, airborne, and ground-based datasets (Barrett, 2003). The main component of SNODAS is the physically based energy-balance and mass-balance NOHRSC Snow Model (NSM) which estimates snowpack parameters at a 1 x 1 km spatial resolution and an hourly temporal resolution (Carroll et al., 2006). SNODAS assimilates available remote sensing data into NSM using a nudging technique to adjust the estimated snowpack parameters, including SWE (Clow, Nanus,

Verdin, & Schmidt, 2012). Daily SWE estimates are expressed as a grid of point estimates in longitude/latitude coordinates with a 1 x 1 km spatial resolution and no real areal extent.

SNODAS data from the winter seasons between October 2013 and April 2018 were used in this study and were projected to an Equal Area Scalable Earth (EASE) grid and subset spatially to the Red River basin.

3.3.2.2 Globsnow SWE Data

The Globsnow project was initiated by ESA in 2008 with the goal of creating a long-term dataset for snow cover extent and SWE for large scale climate research with the second version (used in this study) produced in 2014 (Luojus et al., 2010; Luojus et al., 2014). Globsnow SWE is a coarse resolution (25 km grid scale) product produced by comparing simulated T_b values from the forward Helsinki University of Technology (HUT) snow emission model to observed T_b values retrieved by PM satellites via a cost function (Pullianen, 1999). The HUT model uses a constant snow density of 0.24 g/cm^3, a value determined globally suitable by Sturm et al. (2010). A mountain mask criterion that selects all 25 km grid cells with a height standard deviation greater that 200 m is applied to filter out all pixels classified as mountains (Takala et al., 2011). The final output is a daily SWE map with a 25 x 25 km spatial resolution for the entire Northern Hemisphere projected to an EASE grid. A full description of the processing required to produce Globsnow is available by Takala et al. (2011).

Daily Globsnow SWE estimates are available from 1979 to present and can be freely downloaded from the Finish Meteorological Institute (FMI) in partnership with ESA. In this study, the data from the five winter seasons in question is used.

3.3.2.3 Global Historic Climatology Network - Daily data

The Global Historic Climatology Network (GHCN) Daily dataset provided by the National Oceanic and Atmospheric Administration (NOAA) consists of daily meteorological data from over 80 000 surface stations across the globe. The GHCN-Daily dataset is the most complete daily *in situ* dataset within the United States and is the official archive for the Cooperative Observer Network (COOP) daily data (Menne, Durre, Vose, Gleason, & Houston, 2012).

The GHCN-Daily dataset was used for validation of the downscaled results. Only stations including snow depth measurements within the Red River basin were used for the validation analysis. **Table 3.1** shows the number of in situ measurement stations available within the Red River basin for each season. SWE estimates were calculated by multiplying the snow depth measurements by 0.24 g/cm^3, the same value used in the Globsnow processing.

Table 3.1: Number of in situ SWE measurement locations for each season

Winter Season	Number of *in situ* Stations
2013-2014	27
2014-2015	22
2015-2016	37
2016-2017	37
2017-2018	44

3.3.2.4 Land Cover Data

The land cover class dataset MCD12Q1, developed from Moderate Resolution Imaging Spectrometer (MODIS) data, is used in this study to subset the pixels by land cover. Only coarse

resolution pixels within the Red River basin classified as cropland from the MCD12Q1 dataset were downscaled using RD since over 80% of the region is cropland and to limit uncertainties deriving from land cover variability. MCD12Q1 is a global land cover dataset distributed annually by the United States Geological Survey (USGS) (Friedl et al., 2002). Five land cover schemes are provided in the MCD12Q1 dataset, each developed by different research groups (Friedl et al., 2010). The land cover classification used in this study is the International Geosphere-Biosphere Program (IGBP), a 17-class global land cover scheme produced by Loveland & Belward (1997). The algorithm developed to produce the MCD12Q1 dataset includes 135 input features complied from 32-day averages of reflectance, enhanced vegetation index (EVI) and land surface temperature (LST) data as well as yearly minimum, maximum and mean values of reflectance, EVI and LST. The yearly land cover class data is gridded in a sinusoidal projection with a 500 x 500 m^2 spatial resolution, however, was re-projected to an EASE grid to mask the coarse resolution SNODAS and Globsnow data.

3.3.2.5 Covariate Datasets for Regression Downscaling

Covariate datasets are used in RD to assist in estimating the spatial variability of SWE in the downscaled result. The covariates chosen in this study were satellite-derived datasets available at the target resolution of 1 x 1 km or finer that help describe the variability of SWE.

Local SWE variability can be explained by variables such as microtopography and vegetation (Derksen, Walker, Goodison, & Strapp, 2005; Neumann et al., 2006; Sturm et al., 2010), and therefore, datasets aiding in explaining these phenomena were selected. Four auxiliary variables were chosen as covariates for this study: snow cover extent, land surface

temperature (LST), normalized difference vegetation index (NDVI) and elevation. Snow cover extent and LST datasets are variable throughout the season while the NDVI and elevation data were constant through the season. When possible, composites were used instead of daily values to remove the effect of cloud cover on the downscaled results.

MODIS eight-day snow cover extent data (MOD10A2) with a spatial resolution of 500 x 500 m^2 was downloaded from NSIDC. Daily snow cover is derived from the normalized difference snow index (NDSI) which uses the difference in reflectance properties between visible bands and shortwave infrared band. A pixel in the MOD10A2 dataset is classified as snow if that pixel is snow covered during any of the eight days included in the composite from the NDSI. In this study, all MOD10A2 data from five winter seasons were used and re-projected to the EASE grid.

The MODIS eight-day LST dataset (MOD11A2) is available from USGS with a 1 km spatial resolution and a sinusoidal projection. The eight-day composite is created by averaging the LST values observed from the daily MOD11A1 product. All data from the five winter seasons were re-projected to an EASE grid.

MODIS 16-day NDVI composite data (MOD13A2) was also downloaded from USGS with a spatial resolution of 1 x 1 km. The composite is produced by selecting the best pixel value within the 16-day period, based on a set of criteria including cloud cover, incident angle and the NDVI value. In this study, the MOD13A2 data from a date prior to the beginning of each snow season (mid-October) was used to give a representation of vegetation in the study region. The MOD13A2 data used were re-projected from a sinusoidal projection to an EASE grid.

Shuttle Radar Topography Mission (SRTM) digital elevation model (DEM) data distributed by USGS at a 30 x 30 m^2 spatial resolution (SRTM30) for the United States was used for the static elevation data in the RD algorithms. SRTM30 is an enhanced version of the original DEM dataset obtained from the 11-day SRTM flown in February of 2000 produced by combining USGS Global Topographic Data (GTOPO30).

3.3.3 Data Processing

To downscale the source variable to a target spatial resolution of 1 x 1 km, all covariate datasets are needed at that target spatial resolution. Therefore, the MOD10A2 snow cover extent and SRTM DEM covariates were aggregated to a 1 x 1 km spatial resolution. MOD10A2 was aggregated to a proportional snow cover dataset, and the DEM was aggregated by calculating the mean elevation within the 1 x 1 km grid cell.

The regression models were formulated at the source spatial resolution of 25 x 25 km. Therefore, a coarse resolution version of each covariate was also created. MOD10A2 was aggregated to a proportional snow cover dataset at a 25 x 25 km spatial resolution, where the frequency of snow-covered 500 x 500 m grid cells divided by the total number of 500 x 500 m grid cells within a 25 x 25 km grid cell was calculated. All other quantitative datasets were aggregated using the median value within every coarse resolution grid cell to minimize the influence of outliers. The land cover dataset was aggregated using the mode value within each 25 x 25 km Globsnow grid cell to ensure the most represented land cover within each grid cell was selected. The coarse resolution datasets were then masked by the aggregated land cover dataset, and only up-scaled grid cells classified as cropland (93% of Globsnow pixels) were used for the formulation of the regression models.

The length of the five winter seasons between October 2013 and April 2018 were determined by assessing the Globsnow SWE data. Only dates within each season that Globsnow estimated at least 5 mm of SWE within a minimum of 30 grid cells within the Red River basin were used. The threshold of 5 mm of SWE was chosen based on the knowledge that satellite PM RS observations have difficulty estimating low amounts of SWE and a minimum of 30 grid cells was required to formulate the regression models at the 25 x 25 km spatial resolution. The date range for each winter season is shown below in **Table 3.2**.

Table 3.2: Date ranges for each winter season in study period

Winter Season	Date Range	Number of Dates
2013-2014	2013-12-21 - 2014-04-23	114
2014-2015	2015-01-24 - 2015-04-27	83
2015-2016	2016-01-04 - 2016-04-17	89
2016-2017	2016-11-21 -2017-05-19	165
2017-2018	2017-10-30 -2018-04-30	172

3.3.4 Implementation of Regression Downscaling

To determine the optimal RD method for downscaling coarse resolution Globsnow SWE estimates in the Red River Basin, a “closed loop” experiment was conducted using SNODAS SWE data to test each regression method. As a closed loop experiment, the downscaled results are evaluated by comparing them to their original counterparts. SNODAS SWE estimates for the Red River basin in all five winter seasons were aggregated to a 25 x 25 km spatial resolution using bilinear interpolation, and each RD method (MLR, RFR and GWR) was applied to

downscale the aggregated SWE estimates back to the original 1 x 1 km spatial resolution. The downscaled SNODAS predictions were compared back to the original SNODAS estimates to determine the optimal RD method. Only the days within each season where Globsnow observed at least 5 mm of SWE in a minimum of 30 grid cells was used in this experiment to keep the dates consistent for the implementation of RD to Globsnow SWE data. The formulation of the three regression models was done in R version 3.5.1 (R Core Team, 2018) with the use of *spgwr* (Roger Bivand & Danlin Yu, 2017) and *randomForest* (Liaw and Wiener, 2002) packages, and distinct daily models were produced for each day in the season. Thus, the regression models represent the relationship on each specific day. The bandwidth (or window) parameter required for GWR was specified to include the nearest 30 neighbours of the regression point (grid cell) *i*, to ensure that a reasonable number of observations were included for the generation of the weighted linear regression formula for each grid cell. The default setting for the implementation of RFR were used as they have been acknowledged as reliable parameters and changed in them do not significantly change prediction results (Liaw & Wiener, 2002). Once each daily model was produced, the same regression models were applied to the covariates at the 1 x 1 km spatial resolution for the same day to predict SWE per 1 x 1 km grid cell.

The downscaled SNODAS SWE estimates were compared to the original SNODAS SWE estimates at a 1 x 1 km spatial resolution to assess which method performed best within the study region. Statistical comparisons between the methods and an error analysis was completed to determine the optimal RD method which was then applied Globsnow data for the same study region and study period as the closed loop experiment.

3.3.5 Evaluation of Downscaled SWE

The downscaled results at the target resolution of 1 x 1 km from the Globsnow SWE data were evaluated using both SNODAS data and the GHCN-Daily *in situ* data obtained from NOAA. SNODAS was chosen as a validation dataset in conjunction to the GHCN-Daily dataset given the inherent differences between point data and gridded data and the uncertainties associated with using *in situ* data for validation (S. Wang et al., 2016). Furthermore, SNODAS has been used in numerous studies as validation for PM SWE products (Tedesco & Narvekar, 2010; Vuyovich, Jacobs, & Daly, 2014; Wrzesien et al., 2017).

Both daily error metrics and seasonal error metrics were calculated. Seasonal root mean square error (RMSE), mean absolute error (MAE) and mean bias error (MBE) were calculated by comparing every downscaled predicted SWE grid cell to the matching SNODAS grid cell for each season. Daily basin-wide RMSE values were also calculated by comparing downscaled predicted SWE grid cells with the matching SNODAS grid cells for each day, resulting in a time series of RMSE values throughout the seasons to allow for a temporal analysis of the error to be performed.

Seasonal RMSE and MBE maps were created by subtracting the downscaled predicted SWE grid cells from the SNODAS grid cells on each day and calculating errors on a per pixel basis. These maps, along with season wide downscaled average SWE maps allow for the spatial distribution of the error and SWE to be examined throughout the season.

The downscaled results were also validated using GHCN-Daily in situ data SWE values from NOAA. Daily RMSE, MAE and MBE values were calculated by comparing the in situ SWE value to the predicted downscaled SWE value that the in situ point is located in. Season-

wide in situ bias and RMSE maps were also created following the same process as the SNODAS-derived error maps, however, resulting in point error values instead of pixels.

3.4 Results

3.4.1 Regression Downscaling of Up-scaled SNODAS SWE Estimates ("closed loop" test)

Three regression techniques, MLR, RFR and GWR, were implemented on up-scaled SNODAS SWE estimates and the fine resolution SWE predictions were compared to the original SNODAS SWE values to determine the optimal RD method for this region. The seasonal error metrics are shown in **Table 3.3**, where every downscaled SNODAS pixel throughout a winter season was compared to the corresponding original SNODAS grid cell to obtain one single error metric for the season. Overall RMSE and MBE values for each regression technique are also shown in Table 3.3. The season wide RMSE and MBE values differ between the three methods, with RFR outperforming the other two methods in RMSE in all winter seasons. Over the full five-year period, RFR RD also produced a lower RMSE than the other two techniques. In the 2014-2015 and 2016-2017 seasons, the RFR MBEs are higher than the other three seasons, however, the largest MBE value of 5.4 mm is still considered reasonable. The higher MBE values in the 2014-2015 and 2016-2017 seasons can be explained through a per pixel comparison in **Figure 3.3**. The predicted SNODAS SWE values at 1 x 1 km were compared with the original SNODAS SWE estimates per pixel for each method. It is depicted that RFR is much more concentrated on the 1:1 line with less variation and a higher Pearson's correlation, R, than GWR and MLR for all five seasons. In the 2014-2015 season, all methods are concentrated slightly above the 1:1 line, indicating a positive bias for all three methods, however, for the MLR and GWR methods, there is also much more variability on either side of the 1:1 line, which would

bring the bias closer to 0. In the 2016-2017 seasons, RFR values are again slightly above the 1:1 line resulting in the positive bias whereas both MLR and GWR are much less concentrated along the 1:1 line.

Table 3.3: Average error metrics from closed loop downscaling for each season

	2013 – 2014		**2014 – 2015**		**2015 – 2016**		**2016 – 2017**		**2017 – 2018**		**All Seasons**	
Model	RMSE (mm)	MBE (mm)	RMSE (mm)	MBE (mm)	RMSE (mm)	MBE (mm)	RMSE (mm)	MBE (mm)	RMSE (mm)	MBE (mm)	RMSE (mm)	MBE (mm)
MLR	31	1.5	14	1.2	14	-2.0	37	1.6	16	0.1	30	1.0
RFR	20	0.6	12	2.5	13	-0.6	25	5.4	14	0.2	18	1.8
GWR	29	0.7	13	0.7	14	-2.0	30	0.3	15	0.5	23	0.4

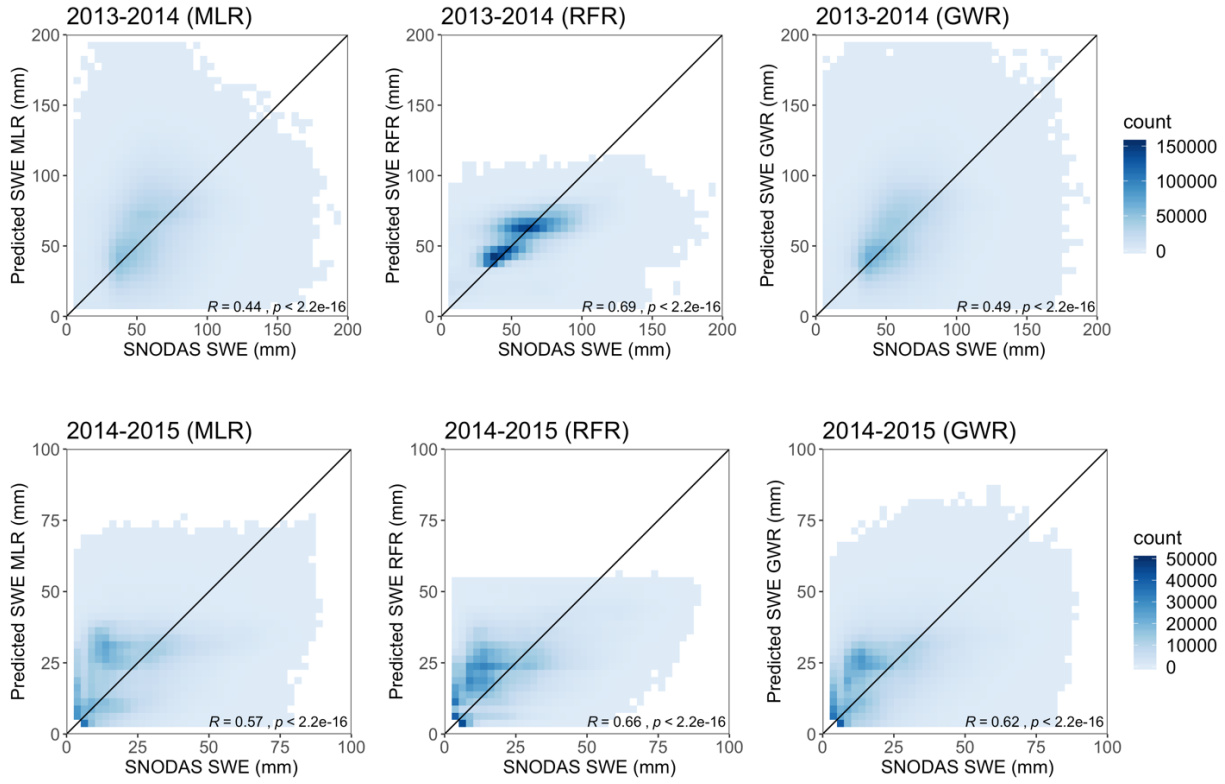

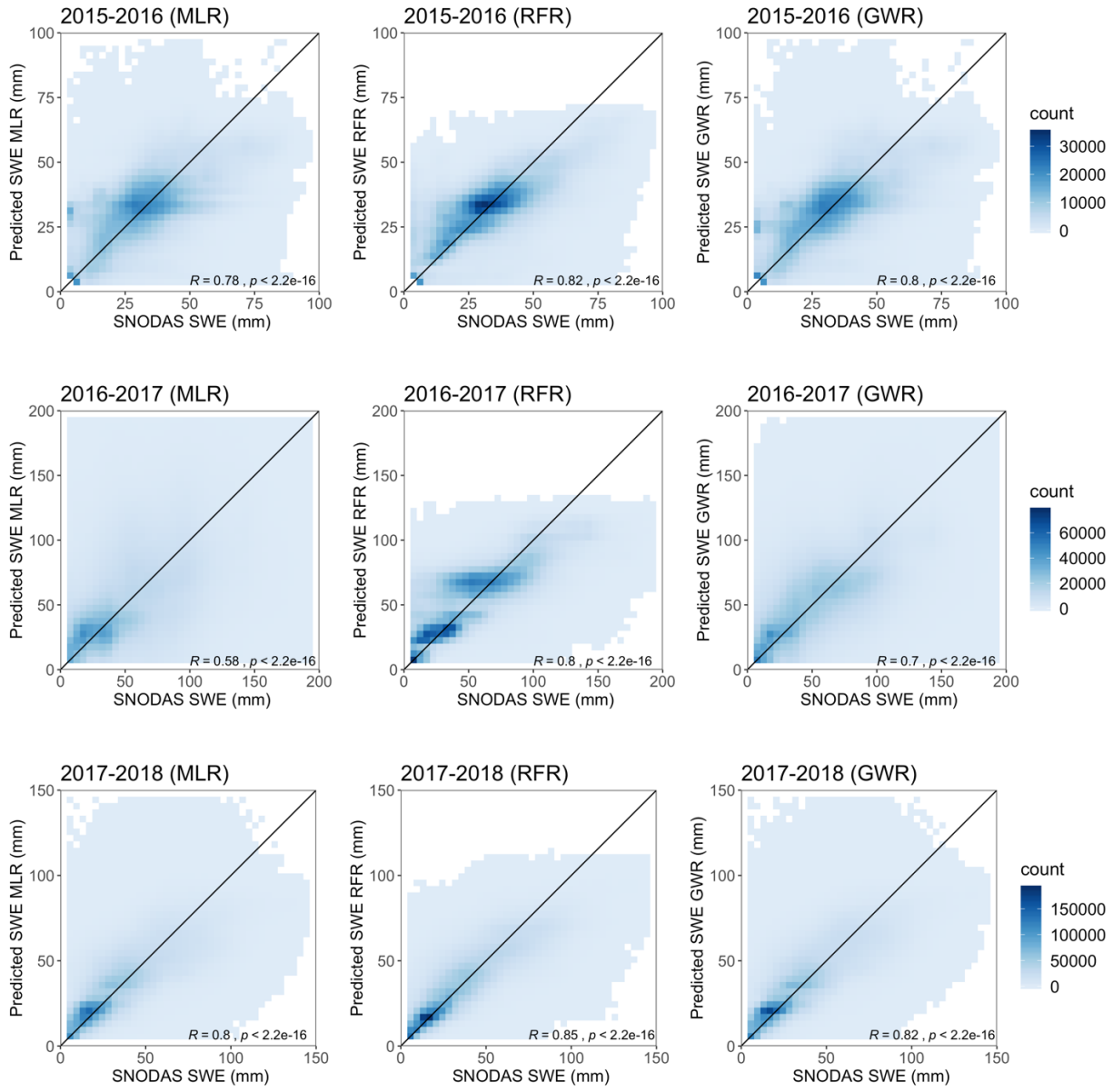

Figure 3.3: Density plots comparing per pixel values of predicted downscaled SNODAS SWE and original SNODAS SWE for each regression method and season

Daily RMSE values for the downscaled SNODAS results throughout the two seasons were also examined in **Figure 3.4**. RMSE values increase through the seasons for each method with higher RMSE occurring at maximum SWE values. In the 2015-2016 winter season, the SWE onset date, formulated from the Globsnow data as mentioned above, is much later than the

2017-2018 season, resulting in a shorter time series. The 2015-2016 season also sees an earlier drop in RMSE values, which corresponds to the snow season occurring earlier in the 2015-2016 season than the 2017-2018 season. In both seasons, RFR (denoted by the orange points) experiences lower RMSE values visually in certain parts of the season. It is noted that when the RMSE is small (~<5mm) which corresponds to small SWE values, the difference between methods is negligible.

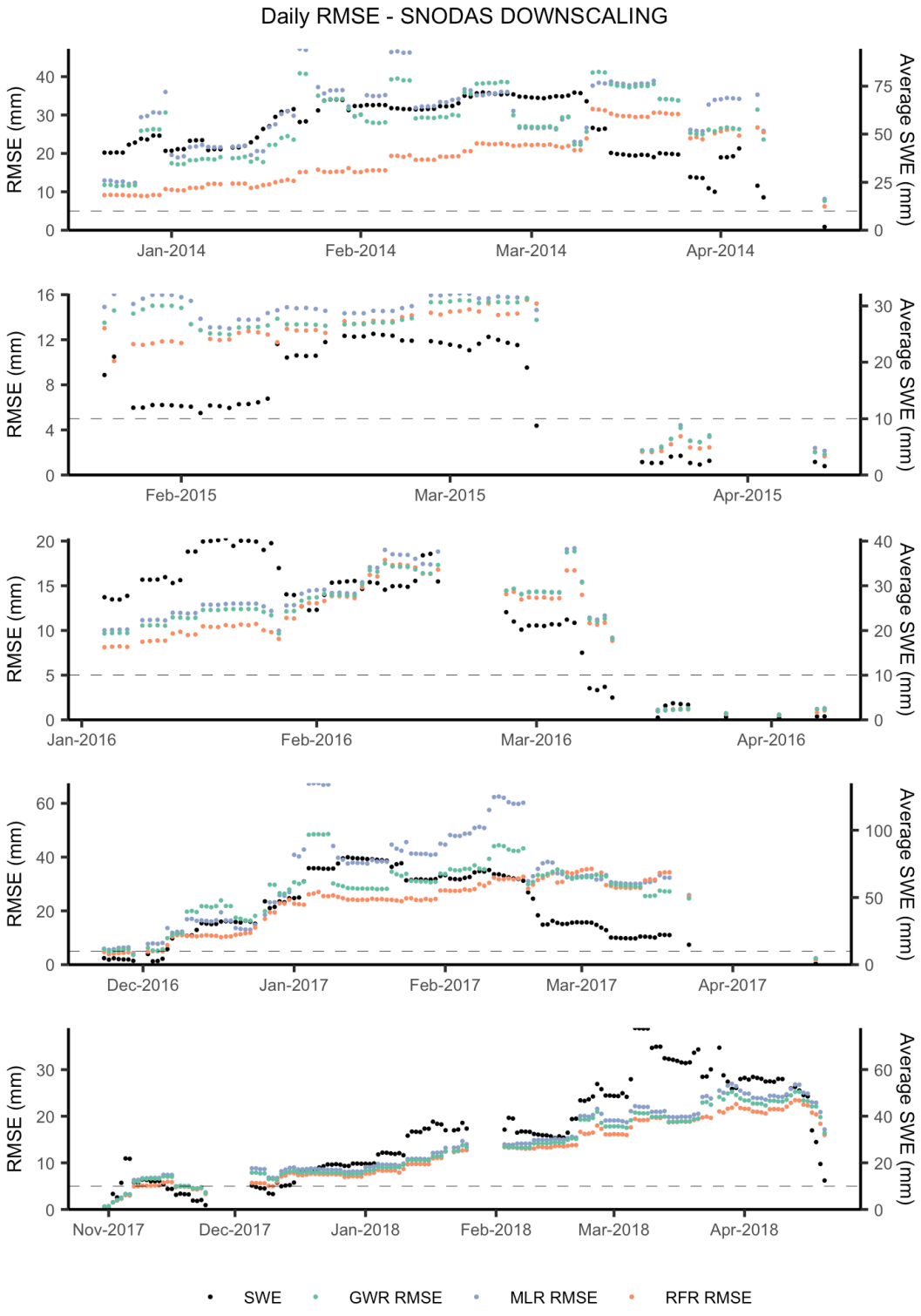

Figure 3.4: Time series of daily RMSE values for the entire basin for all winter seasons

To further assess the three RD methods, one sided T-tests were conducted to determine if there were statistically significant differences between the three daily RMSE values derived from the three regression methods with the results shown in **Table 3.4**. Only days with an average SWE greater than 10 mm were included in the comparison, since the methods show similar results when low amounts of SWE are present (from **Figure 3.4**). Results show that RFR has a lower mean daily RMSE and ($p<0.05$) when compared to MLR for all five seasons and a lower mean daily RMSE ($p<0.05$) when compared to GWR for the 2013-2014, 2014-2015 and 2016-2017 seasons.

Table 3.4: P-values for one sided T-tests comparing daily RMSE between all methods

	M>R	M>G	G>R	G>M	R>M	R>G
2013 – 2014	**>0.05**	0.02	**>0.05**	1	1	1
2014 – 2015	**>0.05**	**>0.05**	**>0.05**	1	1	1
2015 – 2016	**>0.05**	0.1	0.01	0.9	1	1
2016 – 2017	**>0.05**	**>0.05**	**>0.05**	1	1	1
2017 - 2018	**>0.05**	0.2	0.07	0.8	1	0.9

From the examination of **Table 3.3**, **Figure 3.3**, **Figure 3.4**, and the t-test results, it is shown that RFR performs better overall than MLR and GWR across the full study period. Therefore, for the examination of the feasibility of RD to the original and corrected Globsnow SWE datasets, only RFR RD was examined.

3.4.2 Random Forest Regression Downscaling of Globsnow SWE

RFR RD was applied to the original Globsnow SWE data for the five winter seasons between October 2013 and April 2018. Similar to the analysis of the SNODAS RD downscaling experiment in section 4.1, season-wide and daily error metrics were produced by comparing the

downscaled Globsnow results to the original SNODAS data. Furthermore, the downscaled SWE results were also compared to GHCN-Daily in situ measurements. The spatial distribution of error was also examined throughout the season through RMSE and bias maps. **Table 3.5** displays the season-wide error metrics for the downscaled Globsnow SWE data when compared to SNODAS SWE, and **Table 3.6** shows the season-wide error metrics when compared to GHCN-Daily SWE. Smaller error metrics are seen when compared to SNODAS, with an overall RMSE of 21 mm for all seasons. A discrepancy between years exists in error values, with the 2014-2015 season having the lowest errors and the 2017-2018 season having the highest errors in both **Table 3.5** and **3.6**. This corresponds to the length of the snow season, shown in **Table 3.2**. The 2014-2015 season has the shortest season with 83 days ranging from January 4 to April 17, and the 2017-2108 season having the longest season with 172 days ranging from October 30 to April 30. To examine the in-season temporal distribution of SWE, the downscaled SWE is compared to SNODAS SWE and GHCN-Daily SWE in **Figures 3.5** and **3.6** respectively.

Table 3.5: Season wide error metrics for downscaled Globsnow SWE predictions using SNODAS as the reference dataset

Winter Season	**RMSE (mm)**	**MAE (mm)**	**MBE (mm)**
2013 - 2014	31	24	16
2014 - 2015	13	10	2
2015 - 2016	25	19	13
2016 - 2017	45	35	24
2017 - 2018	46	38	37
ALL SEASONS	21	16	-1

Table 3.6: Season wide error metrics for downscaled Globsnow SWE predictions using GHCN-Daily as the reference dataset

Winter Season	RMSE (mm)	MAE (mm)	MBE (mm)
2013 - 2014	37	30	-14
2014 - 2015	15	10	-1
2015 - 2016	29	22	-19
2016 - 2017	52	41	-34
2017 - 2018	55	46	-44
ALL SEASONS	37	30	-15

Figure 3.5 shows the basin-wide daily average downscaled SWE values compared to the basin-wide daily average SNODAS SWE values, whereas **Figure 3.6** displays the daily average SWE for downscaled SWE in pixels that GHCN-Daily SWE in situ measurements are present compared to the basin-wide daily average GHCN-Daily SWE measurements.

Both **Figure 3.5** and **Figure 3.6** shows that the downscaled SWE estimates follow a similar pattern as the SNODAS SWE values as well as the GHCN-Daily SWE values for all seasons with higher discrepancies occurring as SWE increases, typically mid to late season. Typically, the basin wide daily averaged downscaled SWE is overestimating SWE when compared to the validation datasets, especially mid to late season. Overall, the basin wide average downscaled SWE values tend to capture the season wide SWE dynamics.

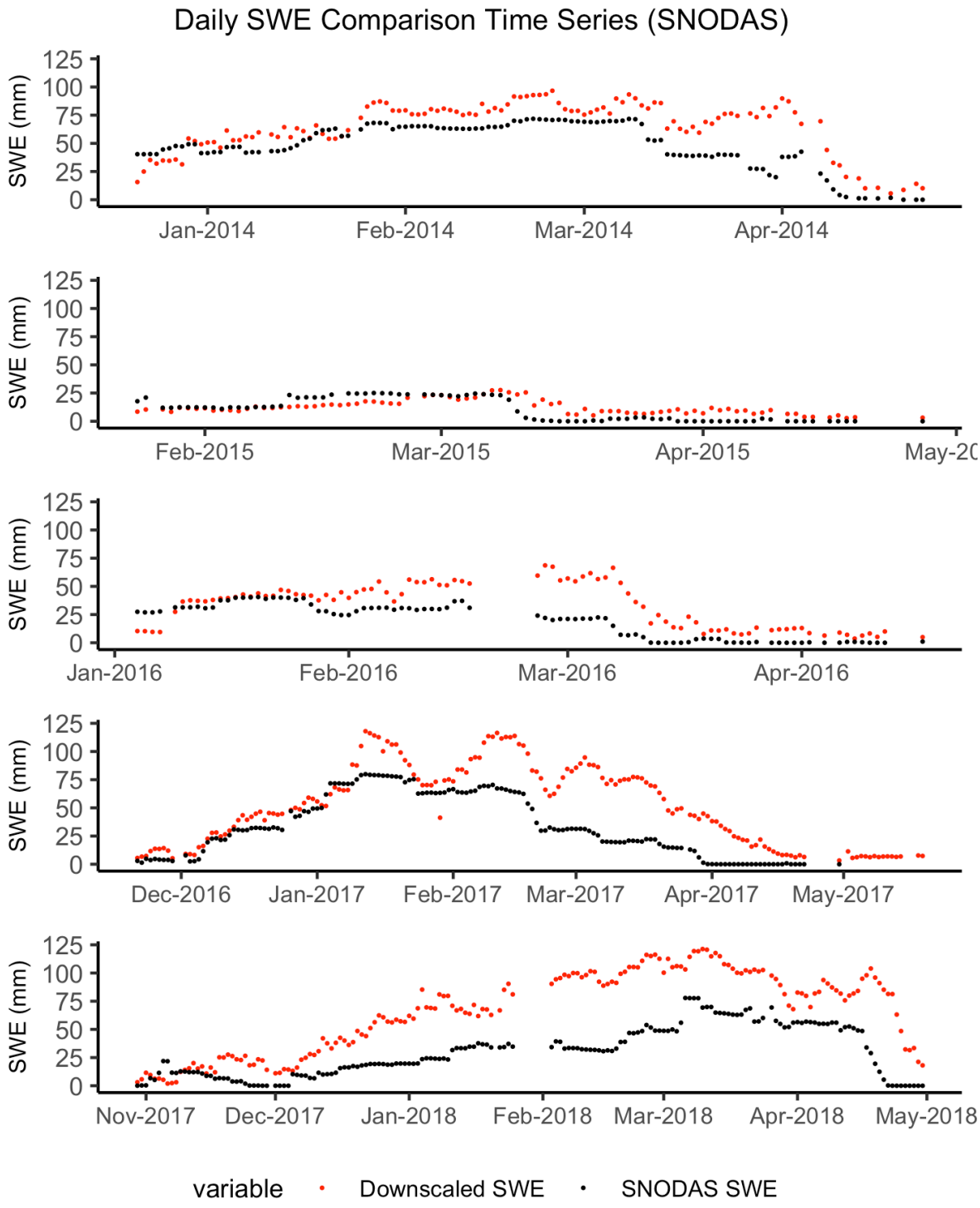

Figure 3.5: Time series of daily average SWE from RFR RD (red) compared to daily average SNODAS SWE (black) for the entire basin

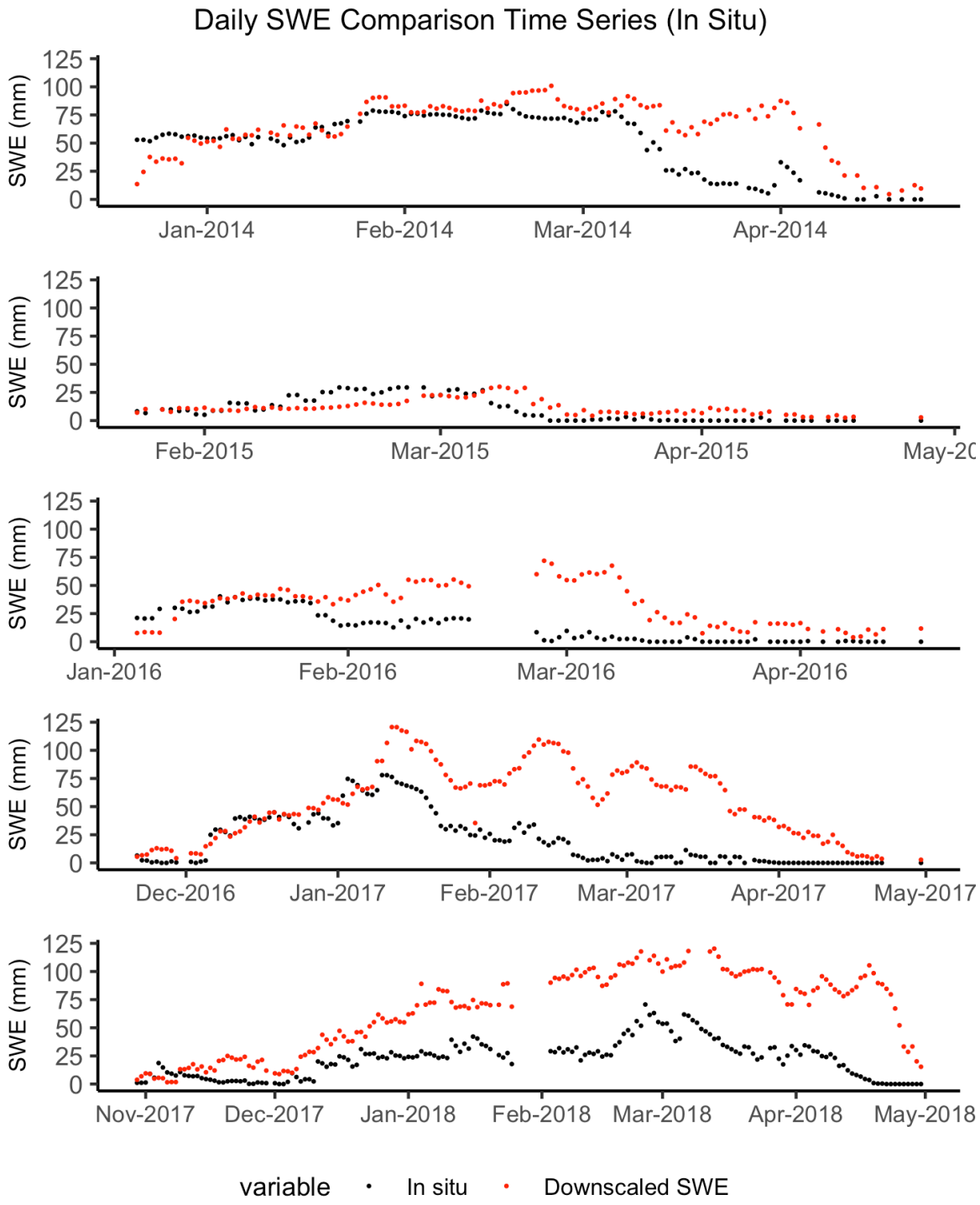

Figure 3.6: Time series of daily average SWE from RFR RD (red) compared to daily average GHCN-Daily in situ SWE (black). Average downscaled SWE is calculated by averaging SWE values for every pixel that an in situ location exists.

Larger differences occur between the daily average downscaled SWE and the GHCN-Daily SWE than when compared to SNODAS SWE, especially later in the snow seasons, where the in situ measurements show a deflating snowpack earlier than the downscaled and SNODAS SWE. The in situ measurements in this region are typically located at airports which are geographically unique sites and not necessarily representative of the surrounding areas; snow accumulation tends to be less in these wind-exposed regions than in non-urban areas which covers the majority of the basin. Therefore, it is likely that the *in situ* dataset underestimates true SWE when averaged over the entire area since it is not representative of the entire basin.

The spatial distribution of error was examined to determine if consistent patterns exist between seasons and to understand the spatial variation and direction of error. Per pixel RMSE, MBE and average SWE maps for each season are shown in **Figure 3.7** for downscaled SWE values, using SNODAS as the validation dataset since the GHCN-Daily in situ measurements are too sparse to examine the spatially continuous error for the entire basin. The per pixel RMSE values show a similar pattern across the seasons, with higher RMSEs occurring in the southern and central portions of the basin, with the exception of the 2014-2015 season where the RMSE values are so low it is difficult to see any pattern occurring. When comparing the RMSE maps to the average SWE maps, there is a clear connection between error and amount of SWE; seasons with higher downscaled SWE estimates are associated with a higher error.

The per pixel bias maps the seasonal time series of average SWE from **Figure 3.5** that the downscaled SWE values typically overestimate SWE when compared to SNODAS, however, areas of underestimation are revealed when examining the results spatially in **Figure 3.7**. In all seasons, except 2017-2018, the downscaled results tend to underestimate SWE in the

northeastern portion of the basin, which is the area that on average acquires the least SWE. Although overestimation is common throughout most of the basin, the downscaled results tend to overestimate SWE more in the southern portion of the basin.

The wavy pattern of error in the basin occurring in all seasons is most likely due to the inherent discrepancies between SNODAS and Globsnow. Since Globsnow is originally produced at a 25 km grid scale, small scale variations in SWE are not as prevalent as SNODAS which is evident at a 1 km grid scale and captures the fine scale variation in SWE better. Therefore, when downscaling Globsnow to a 1km grid scale, although more spatial variation occurs that the original dataset, differences between the two datasets still appear.

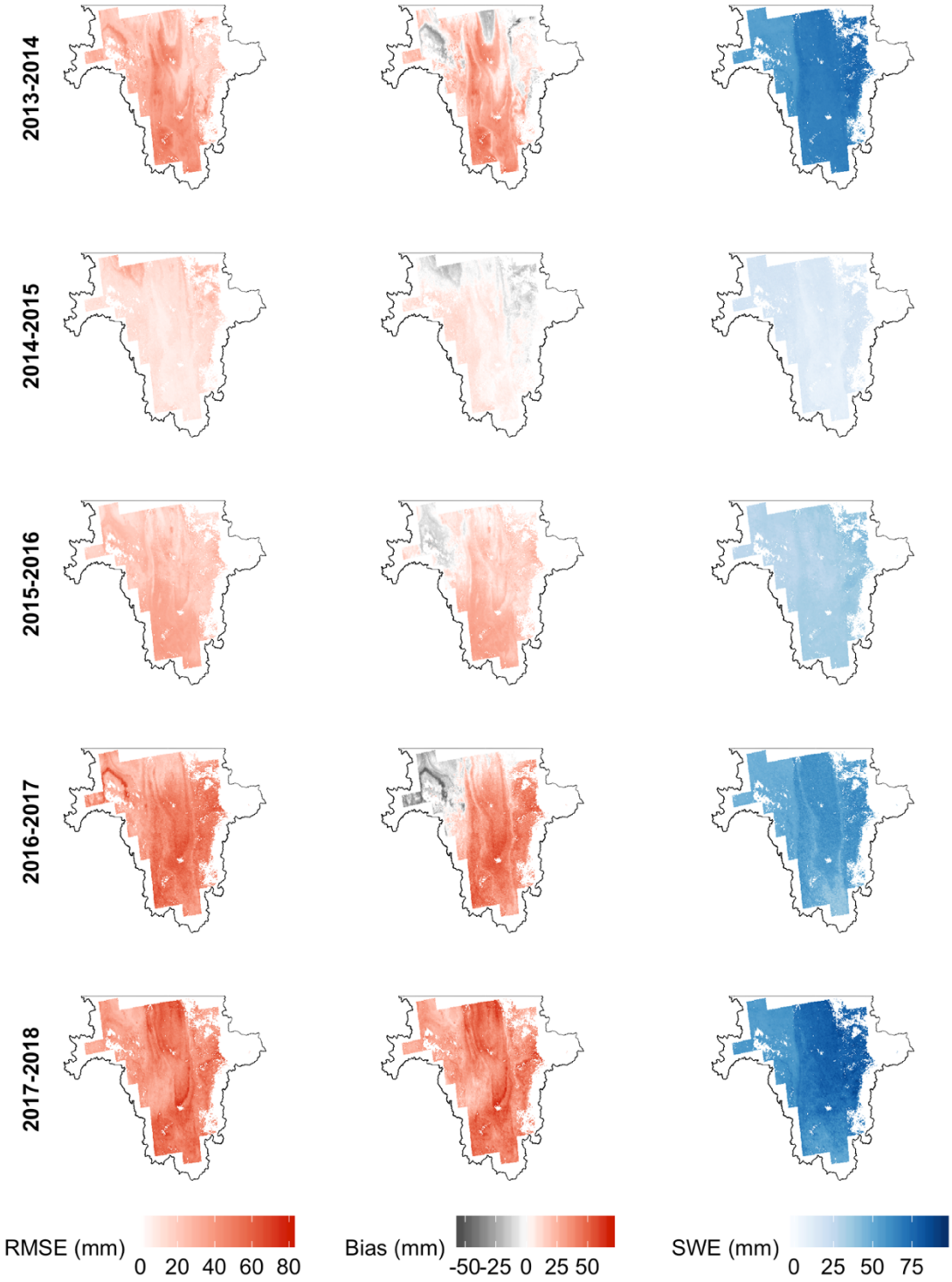

Figure 3.7: Spatial distribution of seasonal RMSE, MBE and average SWE from the downscaled estimates

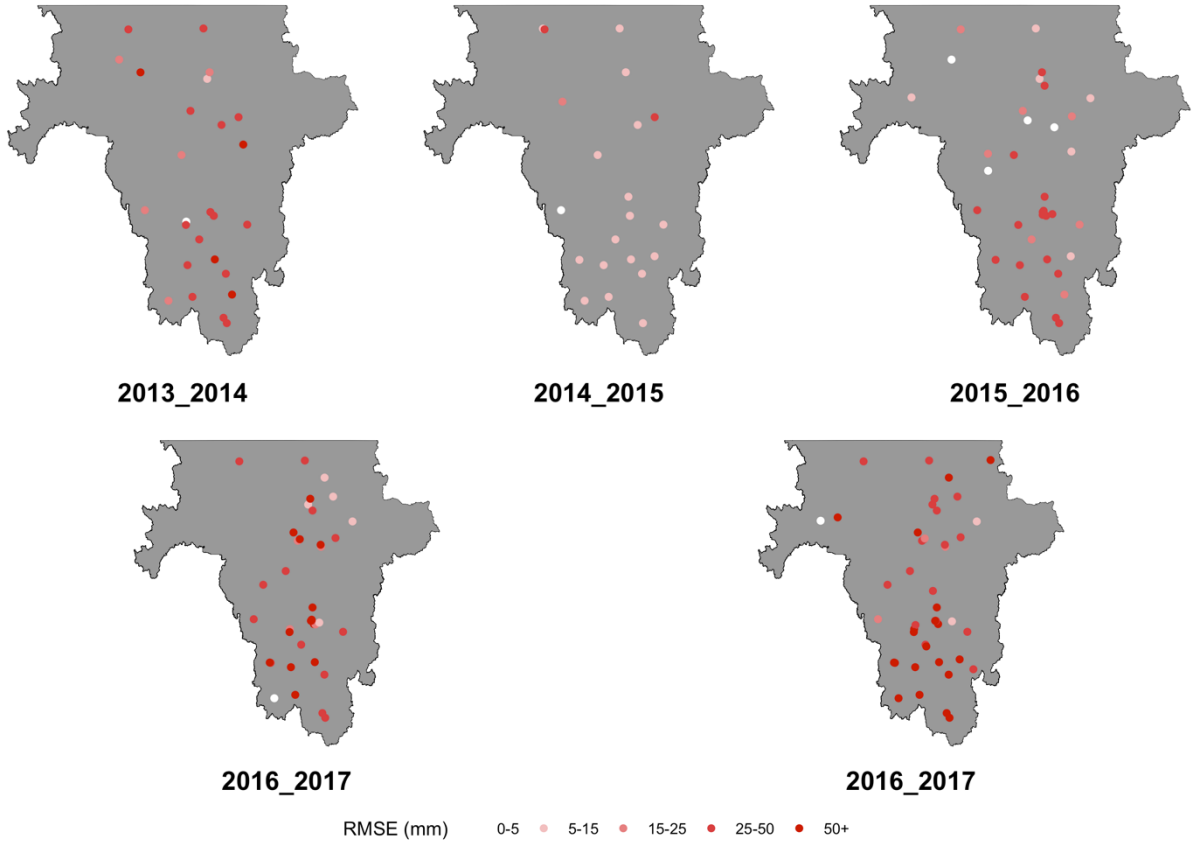

Figure 3.8: Season wide RMSE values at GHCN-Daily in situ stations

The spatial distribution of error calculated by comparing the downscaled results to the GHCN-Daily in situ SWE values was also considered. **Figure 3.8** shows the RMSE value at each in situ location for each season. Similar to **Figure 3.7**, higher RMSE values are found in the 2013-2014, 2016-2017 and 2017-2018 seasons, when higher SWE occurs. With a spatially scarce amount of GHCN-Daily in situ stations, it is difficult to discern any significant spatial patterns of RMSE.

3.5 Discussion

The use of coarse spatial resolution of PM SWE estimates, such as Globsnow, is challenging for local to basin scale applications. This study examines the possibility of using RD methods to increase the spatial resolution of coarse resolution PM SWE estimates such as Globsnow in the Red River Basin. A closed loop RD experiment was applied to SNODAS SWE data to determine the optimal RD method between MLR, RFR and GWR regression techniques. Through this experiment, it was determined that RFR predicted SWE more accurately than both MLR and GWR. One sided t-tests indicated that the daily RMSE values produced by RFR RD were lower than the RMSE values produced by MLR and GWR. Both MLR and GWR assume linear relationships between SWE and the covariates. However, the weaker performances of MLR and GWR suggest that a nonlinear relationship is present, which explains the better performance of RFR. GWR tends to be more reliable for spatial data over MLR given the addition of the spatial relationships of the data, however, the coarse resolution of 25 km is likely responsible for GWR not adding any improvement to the downscaled results. When the GWR model is formulated at a 25 km spatial resolution, the large distance between pixels can result in the weights of surrounding values to be negligible. Therefore, for coarse source spatial resolutions such as Globsnow, using GWR is not useful.

Therefore, RFR was chosen as the optimal RD method and was implemented on a five-year period of coarse resolution Globsnow SWE estimates. An RMSE of 21 mm and 37 mm when using SNODAS and GHCN-Daily in situ measurements as validation datasets, respectively, was found in this study. Overall, it is determined that downscaling Globsnow SWE estimates using RFR RD results in similar errors of those associated with original Globsnow

values. A Globsnow validation analysis in which 1264 in situ locations across the former Soviet Union and Russia and a total of 146 200 samples over a 30 year period is used reports an RMSE value of 43.5 mm and a bias of +2.3mm (Luojus et al., 2014). It is also reported that when incorporating a SWE threshold of 150 mm, which is similar to the SWE values found in this study, the RMSE is lowered to 32.5 mm and the bias is increased to +9.8 mm (Luojus et al., 2014). A recent study by Larue et al. (2017) also examined the accuracy of Globsnow in Eastern Quebec in multiple land classes over a 30-year period (1980-2009). An RMSE of 36.4 mm was reported in open areas covered with croplands, similar to the landscape of the Red River basin, for the months of January and February over the 30-year period.

The downscaled Globsnow SWE results tend to overestimate SWE when compared to the SNODAS and GHCN-Daily reference datasets (**Figures 3.5 and 3.6**). However, it is possible that both the reference datasets are underestimating SWE, particularly at the end of the season when the overestimation of downscaled SWE is largest. As mentioned in **Section 3.4.2**, the majority of the GHCN-Daily measurements are located in airports or urban areas, which typically experience less snow accumulation than surrounding rural areas. The SNODAS SWE assimilation incorporates in situ measurements to estimate gridded SWE, implying that the uncertainties associated with in situ measurements in this region are transferred to the SNODAS estimates. The limited studies that have assessed the accuracy of SNODAS tend to examine mountainous regions (e.g. Anderson, 2011; Clow et al., 2012) and are difficult to compare to the cropland landscape in the Red River basin. Therefore, a further work is required to understand the reliability of the reference datasets used in this study.

Further analysis is also recommended to better understand RD in different locations, across different land cover types and with added covariates. It has been concluded that certain land cover classes can increase the error of PM remote sensing-derived SWE estimates (Chang et al., 1996). In forested regions, for example, the observed PM signal is comprised of both the signal from the forest canopy, as well as the underlying snowpack, resulting in an underestimation of SWE (Cohen et al., 2015; Kruopis et al., 1999; Kurvonen & Hallikainen, 1997). Thus, testing the feasibility of RD in areas of different land classes is crucial in determining the spatial coverage of this method.

The covariates used in this study were chosen based on availability and applicability to SWE, however, it is known that additional variables such as location (longitude/ latitude), day of year, air temperature and precipitation patterns play a significant role in the accumulation and redistribution of snow in certain landscapes (Neumann et al., 2006; Sexstone & Fassnacht, 2014). Therefore, future studies should examine the feasibility of expanding the number and derivation of covariates used in RD on coarse resolution Globsnow SWE estimates to more accurately describe the variability in SWE across the basin.

A further consideration for the accuracy of RD is the assumption of that the regression model formulated at the source spatial resolution is valid at the target resolution. RD fundamentally assumes that the relationship formulated at the source spatial resolution of 25 x 25 km, in this study, is constant through all spatial resolutions. Although the assumption is needed for this method to be implemented, in reality, relationships between variables can change with spatial scale. It is possible that the relationship between SWE and the covariates used may vary at different scales since different physical processes are at play. To understand the between-scale

variation in the relationship between SWE and the covariates used in this study, it is suggested that an in-depth examination is conducted to compare these datasets and their relationships at varying spatial scales in the Red River basin. It is possible that there is a target spatial resolution threshold in which downscaling coarse resolution Globsnow SWE estimates should not be implemented past, however, this information is currently unknown.

Additional error may be induced when upscaling the covariates the 25 x 25 km spatial resolution for regression formulation. For example, when elevation is up-scaled to 25 x 25 km grid cells from 30 x 30 m grid cells using the median value within the coarse resolution grid cell, the fine scale variations in the landscape are not being considered and the regression model is being formulated using elevation values that may not be representative of each 25 x 25 km grid cell.

Despite the drawbacks identified above, results show that RFR RD is a feasible approach for downscaling Globsnow SWE estimates to a fine resolution in the Red River basin without increasing significant error. A further improvement to the RFR RD used here, would be to account for spatial correlation in the modelling. Downscaling coarse resolution gridded data is inherently a spatial problem, and the spatial correlation may play an important role. Therefore, further work should test other methods that include spatial correlation, such as Area to Point Regression Kriging (ATPRK) (Atkinson, 2013). ATPRK combines kriging downscaling methods with regression downscaling to reduce disadvantages associated with both methods individually. ATPRK has been recently implemented with success to downscale land cover and soil moisture gridded datasets, however, no studies have examined this method for downscaling

SWE data (e.g. Jin, Ge, Wang, Heuvelink, & Wang, 2018; Wang, Shi, Atkinson, & Zhao, 2015 and others).

3.6 Conclusion

This study examined the potential of using RD to downscale coarse resolution PM SWE estimates from a 25 x 25 km spatial resolution to a 1 x 1 km spatial resolution. Three regression techniques (MLR, RFR and GWR) were implemented and assessed and it was determined that for this study region and period, the use of RFR RD was the most accurate approach as both MLR and GWR approaches produced higher errors. It is noted that GWR may be more acceptable if downscaling a higher resolution source dataset, as the difference between the source resolution and the target resolution becomes smaller and more variation in the GWR model exists throughout the study region. Overall, RFR RD is considered a feasible approach to decreasing the pixel size of Globsnow SWE estimates in the Red River basin over a five-year period from October 2013 to April 2018, without increasing the errors typically found in the original Globsnow dataset.

This study can help to better understand the use of PM remote sensing-derived SWE estimates for local scale applications. Currently, such estimates are only suitable for regional to global applications, however, with RD it is possible to gain knowledge on seasonal SWE dynamics at local scales. In the absence of higher spatial resolution SWE, this approach could be beneficial for local communities in flood-prone regions in preparing for and mitigating damages due to rapid springtime flooding. The Red River basin is an area with a long history of spring

flooding due to snowmelt and with this information, economic and agriculture infrastructure can be protected.

Chapter 4 Discussion and Conclusion

4.1 Summary

The availability of daily, global satellite PM RS SWE estimates through products such as Globsnow are beneficial for understanding the dynamics of large scale hydrological and climatological systems. However, the coarse spatial resolution of the Globsnow SWE product hinders its use for local to regional scale applications. Downscaling methods such as RD have been successfully applied to increase the spatial resolution of gridded satellite datasets such as LST, precipitation and soil moisture, however, limited work has focused on the implementation of RD to coarse resolution SWE estimates. Therefore, this research focuses on the use of RD to increase the spatial resolution of satellite-derived coarse resolution SWE estimates from Globsnow to contribute to the need for daily real-time estimates of SWE at a local spatial resolution.

RD is a simple downscaling method that uses the relationship between the desired source variable to be downscaled and related covariates. Multiple regression techniques can be applied to best represent the relationship between the source variable and the covariates, making this a versatile approach. Multiple studies have examined the feasibility of multiple RD techniques to other source variables with the best technique differing between studies (e.g. Chen et al., 2015; Duan & Li, 2016; Hutengs & Vohland, 2016; Yu et al., 2008). Therefore, it is suggested that the

best suited RD technique depends on the study region, the source and target resolution and the source variable to be downscaled. To assess RD for SWE applications, this thesis explored the feasibility of implementing RD to Globsnow, a coarse resolution satellite PM SWE product, in the Red River basin through the experimentation of multiple RD techniques.

Three RD techniques were first applied in a closed loop experiment where 1 x 1 km grid cell SNODAS SWE estimates were up-scaled to a 25 x 25 km spatial resolution to match the resolution of Globsnow SWE data, and then downscaled back to the original 1 x 1 km spatial resolution. This closed loop experiment was executed to assess MLR, GWR and RFR RD techniques while removing the uncertainties associated with the use of reference datasets. The downscaled SNODAS SWE estimates were compared to the original SNODAS SWE estimates to assess the coherence between the two datasets, and thus, determine the most reliable RD technique for this study region. Through this experiment, it was determined that RFR RD estimates produces lower RMSE values across all seasons compared to the MLR RD and GWR RD estimates. An overall RMSE of 18 mm was calculated over the full five-year period for RFR RD estimates compared to RMSE values of 30 mm and 23 mm over the same time period for MLR RD and GWR RD estimates, respectively. It was also concluded that RFR RD estimates produced less variation and a higher correlation than MLR RD and GWR RD estimates when comparing each downscaled pixel value to the original pixel value for each season. Through the closed loop experiment analysis, it was determined that overall RFR RD was the most suitable RD technique in this region and, therefore, RFR RD was applied to the same five-year period of Globsnow SWE estimates for the same study region. The downscaled results were compared to the original SNODAS data as well as GHCN-Daily in situ SWE estimates to assess error on both

a spatially continuous and discontinuous field. Overall RMSE values of 21 mm and 37 mm were found when using SNODAS and GHCN-Daily SWE values as the reference datasets, respectively. These RMSE values found in this study are similar to the RMSE values found in validation studies of the original Globsnow SWE dataset ranging from 30-50 mm (e.g. Larue et al., 2017; Luojus et al., 2014), suggesting that implementing RFR RD on Globsnow SWE does not increase error in this study region and period, and could potentially be used for basin scale hydrological and climatological applications.

This study showed that there is potential for RD to successfully downscale coarse resolution Globsnow SWE without an increase in uncertainty occurring. However, there are limitations regarding RD that may induce other errors not easily detected in the evaluation analysis of the downscaled results. These limitations, discussed in the following section, suggest that further work including the examination of other downscaling methods may be of interest to examine for a better representation of seasonal SWE dynamics at the local to basin scale.

4.2 Methodological Limitations

The methodology applied in this thesis has certain limitations that may add to the uncertainty associated with the results. Uncertainties regarding the reference datasets used to analyze the downscaled results as well as limitations regarding the RD method inherently are two main sources of uncertainty within this study.

Two reference datasets were used to assess the performance of RFR RD in the Red River basin. GHCN-Daily, a network of in situ snow measurements, and SNODAS, a gridded data assimilation SWE product, both induce uncertainty in the error metrics produced when used as an evaluation dataset for the downscaled Globsnow SWE estimates. RS data is typically

validated using in situ point measurements, however, the inherent difference between point measurements and grid cell measurements, especially for coarse resolution grids, and the locations of in situ measurements make the representativeness of using point measurements for grid-cell evaluation uncertain (S. Wang et al., 2016). Point measurements only capture a single value at one specific location and do not take into account the variation within a grid cell, potentially leading to an unreliable assessment of RS estimates, especially in coarse resolution grids and/or heterogenous landscapes (e.g. Jackson et al., 2012). The geographical location of in situ measurements also adds to the uncertainty in using them as reference datasets. In situ measurements sites tend to be located in easily accessible, homogenous regions of a landscape and can be extremely sparse over a study domain. In snow research, particularly, it has been found in many studies that permanent in situ measurement locations tend to be taken in clearings, at airports or homogenous areas that are not representative of their surroundings (Derksen et al., 2005; Derksen et al., 2003; Foster et al., 2005). Added uncertainty is produced by using the GHCN-Daily in situ measurements as a reference dataset in this study since only snow depth is directly measured at the in situ locations, and in situ SWE is estimated in this study using a constant snow density of 0.24 g/cm^3 (the same value used in the Globsnow algorithm). Although snow depth tends to be more influential to SWE variability than snow density (Derksen et al., 2005; Sturm et al., 2010), it is likely that density does vary across the study region and that the in situ SWE measurement used as a reference is not exactly true. The spatial coverage of in situ locations in this study is relatively sparse and does not capture the total variation SWE across the region. The number of in situ measurement locations varies between 22 and 44 throughout the five winter seasons. The locations of the sites are congregated along the Red River, where large

communities reside, with many of them located at airports, which may contribute to the over estimation found in the evaluation analysis using the GHCN-Daily SWE values.

To combat the issues regarding using point measurements for evaluation, this study also used SNODAS, a gridded data assimilated SWE product, as a reference dataset. This creates a spatially continuous error analysis, which allows for a better understanding of how the downscaled SWE estimates perform across the entire basin. However, uncertainties regarding the SNODAS SWE estimates also exist. SNODAS is a data assimilated SWE product, combining a physically based energy and mass balance model with data from satellite, airborne and in situ measurements when available. Therefore, SNODAS incorporates in situ measurements where available, resulting in the uncertainties associated with in situ measurements being integrated into the SNODAS estimates. It is unknown, however, when and where additional data is incorporated into the energy and mass balance model. Very few studies have assessed the accuracy of SNODAS SWE estimates, with most of them focusing on mountainous regions where satellite PM SWE estimates are not reliable (e.g. Anderson, 2011; Clow et al., 2012; Hedrick et al., 2015). Moreover, very limited official documentation regarding uncertainty is published with the data since it is an operational dataset and is continuously updated. Therefore, no reliable uncertainty measurement is known for SNODAS in the Red River basin, causing concern for using it as a reference dataset. It is suggested, however, that SNODAS preforms better in areas with a higher density of in situ SWE measurements, in some cases matching in situ SWE measurements perfectly (Wrzesien et al., 2017). A recent study by King, Erler, Frey, & Fletcher (2020) evaluated SNODAS in Southern Ontario and found a positive mean bias of approximately 50% from 2011 to 2017 indicating that overestimation of SWE in SNODAS

estimates is not uncommon. Regardless of these issues surrounding SNODAS, it is still a commonly used reference dataset for assessing the accuracy of satellite PM SWE estimates in many studies (e.g. Tedesco & Narvekar, 2010; Vuyovich et al., 2014; Wrzesien et al., 2017). Given the fairly high number of *in situ* measurement locations within the Red River basin and its non-complex terrain, it is suggested that SNODAS should be a decent reference dataset for this study, however, it is likely that some uncertainties still exist since it is not a direct measurement of SWE. It would be of interest to examine the accuracy of SNODAS SWE estimates in the Red River basin similar to studies such as Hedrick et al. (2015) and King et al. (2020) to gain a quantitative understanding of the uncertainties present in this region. Uncertainties in both the GHCN-Daily in situ measurements and the gridded SNODAS estimates may have severe implications when using them as reference datasets for the downscaled Globsnow SWE results, however, the use of both datasets give a better understanding of the performance since we are not heavily relying on one sole reference dataset.

Limitations regarding the inherent characteristics of the RD approach also add uncertainty to the downscaled SWE estimates. RD is a simplistic downscaling approach that is easily reproducible and relatively versatile, however, limitations regarding the assumptions of stationarity and scale invariance need to be addressed.

Many regression techniques include the assumption of stationarity, implying that the mean and variance of the source variable is constant throughout space, however, in most real-world applications, data are non-stationary (Blöschl, 1999). Therefore, it is conceivable that regression techniques that do not assume stationarity would be more reliable in estimating SWE through RD. This concept lead to the implementation of GWR RD, which can account for the

non-stationarity of SWE in the study domain, however, it was shown in Chapter 3 that GWR was outperformed by RFR for downscaling coarse resolution SWE estimates, and therefore RFR RD was chosen as the superior method.

The problem with using GWR RD in this study is most likely due to the extreme coarse resolution of the source variable and the small spatial coverage of the study site. When generating the regression equation at each coarse resolution pixel, an inverse distance weight is applied to data from surrounding pixels within a set neighbourhood before it is implemented into the model. To generate a reliable GWR equation at a specific Globsnow grid cell, a neighbourhood of at least 30 grid cells surrounding the grid cell in question is required. This creates issues with this specific study region and source variable. Globsnow SWE is originally produced at a 25 x 25 km spatial resolution, meaning the inclusion of 30 surrounding pixels in the neighbourhood can incorporate information from pixels hundreds of kilometers away from the grid cell in which the equation is being generated for. For the Red River basin only 118 coarse resolution pixels are present. Therefore, at least 25% of the total pixels are required to generate the regression equation for each pixel. Thus, small datasets, or in the case of downscaling 25 x 25 km to 1 x 1 km SWE grid cells, small study regions, are not suitable for GWR RD.

The assumption of that the regression model formulated at the source resolution holds at the target resolution applied in the RD method adds further uncertainty to the downscaled Globsnow SWE estimates. During RD, a regression model is formulated at the source spatial resolution to describe the relationship between the source variable and the covariate(s). The source spatial resolution in this study is the resolution of the original Globsnow data which is a

25 km grid scale. The assumption of scale invariance included in the RD method, thus implies that the relationship described by the regression formula at the source spatial resolution holds at the target resolution. Therefore, in this study, it is assumed that the RFR model describes the relationship between Globsnow SWE and the covariates accurately at both the 25 km grid scale and the 1 km grid scale. This assumption, however, may not be true for all scale changes or study sites, and needs further investigation. It may be that at a certain spatial resolution, the relationship between SWE and the covariates used in this study differs, therefore, predicting inaccurate SWE estimates at the target spatial resolution.

The limitations associated with the reference datasets used as well as the RD approach give motivation to assess other evaluation techniques and downscaling methods in further studies. The following section covers recommendations of further work in the field of downscaling coarse resolution SWE estimates for local applicability.

4.3 Recommendations

RD has not been extensively examined as a viable approach to estimate SWE at a higher spatial resolution. The datasets used in this study as well as the advantages and disadvantages associated with RD illustrate possible sources of uncertainty that may affect the reliability and accuracy of the downscaled SWE results. The examination of alternative reference and covariable datasets as well as the consideration of alternative downscaling methods may decrease the uncertainty and give more trustworthy SWE estimates at the local spatial scale.

The issues with reference datasets are difficult to overcome without the availability of a dense spatial coverage of in situ SWE measurements and/or airborne SWE estimates. For the

Red River specifically, airborne SWE measurements provided by NOHRSC are available for select days within the winter seasons of 1988, 1989, 1997, 2018 and 2020. It may be beneficial to test the RFR RD method used in this study on the days in which the airborne data are available to further understand the accuracy and reliability of the downscaled SWE estimates. Studies by Josberger, Mognard, Lind, Matthews, & Carroll (1998), Singh & Gan (2000) and Gan, Kalinga, & Singh (2009) utilize this data for comparison and validation of satellite PM SWE estimates within the Red River basin, exhibiting the benefits of using airborne SWE retrievals for evaluation. In situ SWE measurements are difficult and costly and would require a field campaign to obtain the necessary density of measurements for a reliable validation dataset. A challenge with using airborne or field campaign in situ SWE measurements is the lack of consistent temporal coverage available and thus, the inability to assess the accuracy of the downscaled SWE estimates throughout a winter season.

It may also be beneficial to examine alternative covariate datasets that may assist in better describing SWE within the regression model used in RD. The datasets used in this study were chosen based on availability, satellite derivation and previous studies concluding their influence on SWE. However, relationships may vary across space, landscapes or time and may require alternative covariables for this specific study site. Furthermore, an understanding of the variation of the relationship between SWE and its covariates at differing spatial scales is needed to trust RD as a method.

RD is a straightforward downscaling method that has successfully been used in many RS contexts. However, additional downscaling methods such as area to point interpolation or hybrid approaches exist that may be more suitable for SWE applications. Area to point

interpolation methods such as area to point kriging (ATPK) and downscaling cokriging (DSCK) use a geostatistical framework to downscale coarse resolution remote sensing data. Benefits associated with area to point interpolation approaches are their ability to account for the modifiable area unit problem, incorporation of spatial correlation, unbiased predictions and coherence of the downscaled output (Jin et al., 2018; Kyriakidis, 2004; Q. Wang, Shi, & Atkinson, 2016). Both ATPK and DSCK incorporate the spatial autocorrelation of the source variable to predict values at point locations within the study area. DSCK, being the multivariate form of ATPK, also includes the within and between spatial correlation of related covariables to predict the source variable at point locations. A key component of ATPK is the estimation of a point to point (punctual) semivariogram of the source variable, with the addition of the estimation of punctual semivariograms for each covariable as well as a punctual cross covariogram between the source variable and each covariable for DSCK. The punctual variograms can be estimated through deconvolution techniques, such as the method employed in Q. Wang et al. (2015).

ATPK is computationally simpler than DSCK since the addition of covariables are not involved, however, snow distribution is heavily dependent on external variables, and therefore, ATPK by may be impractical for this application. DSCK, in comparison, allows for the spatial structure of both the source variable and a covariable as well as the joint spatial variability between them to be considered (Pardo-Igúzquiza & Atkinson, 2007). The incorporation of spatial autocorrelation and cross correlation in area to point interpolation methods make them appealing for downscaling coarse resolution SWE estimates. ATPK and DSCK are applicable to RS data since they incorporate the spatial correlation. Further benefits are the coherence between the coarse resolution source variable and downscaled source variable and the ability to

perform uncertainty assessments on ATPK and DSCK predicted results through a Monte Carlo simulation approach (Kyriakidis, 2004).

More recently, area to point interpolation and RD have been combined to produce a hybrid method known as area to point regression kriging (ATPRK) (e.g. Kim & Park, 2017; Teng, Shi, Ma, & Li, 2014; Q. Wang et al., 2015). ATPRK has the benefit of using the advantages associated with one method to reduce the disadvantages of another method in the same downscaling process and has become widely used for downscaling RS data. ATPRK combines regression downscaling and ATPK into one downscaling procedure, allowing for related covariables to be included in the prediction of $\hat{Z}_S(v_T)$ without the extra computational power required for DSCK. ATPRK follows a four step procedure, where 1) regression downscaling is applied on the coarse resolution source variable, 2) coarse resolution residuals are obtained from the regression model formulated in step 1, 3) ATPK is performed on the coarse resolution residuals and 4) the downscaled residuals from step 3 are added to the downscaled predicted source variable from step 1. This approach incorporates the spatial structure of the source dataset, while also accounting for the relationship between the source variable and related covariates. Original ATPRK methods used SLR or MLR models, however, the assumption of stationarity resulted in uncertainties when downscaling RS data. Recent methods such as Adaptive ATPRK (AATPRK) employed by Q. Wang et al. (2016) and the geographically weighted ATPRK (GWATRPK) implemented by Jin et al. (2018) use non-stationary regression techniques remove the assumption of stationarity.

This study employed RD as a preliminary investigation into downscaling coarse resolution SWE estimates since limited work has explored these concepts in regard to SWE.

Results of this study demonstrate that RFR RD performs better than GWR or MLR in the Red River basin when conducting a closed loop experiment on SNODAS SWE, and that RFR RD of Globsnow SWE performs adequately without increasing uncertainty of the original Globsnow dataset. However, it will be beneficial to assess these more complex downscaling methods that may better capture the spatial and non-spatial relationships of the source variable and covariates in a further study and compare the results to the RFR RD SWE estimates found in this study.

4.4 Conclusion

The overall aim of this thesis was to examine the feasibility of downscaling coarse resolution satellite PM SWE estimates. This thesis focused on the implementation of RD as an initial assessment given the simplicity and reproducibility of the method and evaluated its accuracy in the Red River basin, a flood-prone region of northern United States with high agricultural importance. It was determined through a closed loop experiment where fine resolution SNODAS SWE estimates were up-scaled to a 25 km grid scale, and downscaled using three RD techniques, that RFR RD outperformed MLR and GWR RD. RFR RD was then applied to a five-year period of Globsnow SWE estimates in the same study region to produce 1 km grid scale SWE estimates. An evaluation analysis of the downscaled SWE results was completed using 1 km grid scale SWE estimates and GHCN-Daily in situ SWE estimates. It was found that throughout the five winter seasons, the downscaled results typically overestimate SWE and overestimation increases as SWE increases. Overall RMSE values of 21 mm and 37 mm were found when using SNODAS and GHCN-Daily datasets for reference, respectively. These error metrics are within a reasonable range when compared to error metrics found in

validation studies of coarse resolution Globsnow SWE estimate, suggesting that no increase in error occurs with downscaling.

The ability to estimate SWE at the local to basin spatial resolution with continuous daily temporal coverage is crucial for communities in snow induced flood-prone regions around the world. An improved understanding of seasonal SWE dynamics at the local scale will lead to better management of economic, environmental and agricultural changes that are directly influenced by SWE. Further work is needed to assess other downscaling methods, as well as examining downscaling feasibility in varying landscapes to aid in producing a global SWE product with local applicability.

Bibliography

AMAP. (2017). Snow, Water, Ice and Permafrost in the Arctic (SWIPA); Summary for Policy-makers.

Agam, N., Kustas, W. P., Anderson, M. C., Li, F., & Neale, C. M. U. (2007). A vegetation index based technique for spatial sharpening of thermal imagery, *107*, 545–558. https://doi.org/10.1016/j.rse.2006.10.006

Anderson, B. T. (2011). Spatial Distribution and Evolution of a Seasonal Snowpack in Complex Terrain: An Evaluation of the SNODAS Modeling Product, (May), 109. Retrieved from http://scholarworks.boisestate.edu/cgi/viewcontent.cgi?article=1181&context=td%5Cnhttp://scholarworks.boisestate.edu/td/181/

Anderson, M. C., Norman, J. M., Mecikalski, J. R., Torn, R. D., Kustas, W. P., & Basara, J. B. (2004). A multiscale remote sensing model for disaggregating regional fluxes to micrometeorological scales. *Journal of Hydrometeorology*, *5*(2), 343–363. https://doi.org/10.1175/1525-7541(2004)005<0343:AMRSMF>2.0.CO;2

Armstrong, R. ., & Brodzik, M. . (2001). Recent Northern Hemisphere Snow Extent: A Comparison of Data Derived from Visible and Microwave Satellite Sensors. *Geophysical Research Letters*, *28*(19), 3673–3676. https://doi.org/10.1136/sti.2006.023606

Atkinson, P. M. (2013). Downscaling in Remote Sensing. *International Journal of Applied Earth Observations and Geoinformation*, *22*, 106–114. https://doi.org/10.1016/j.jag.2012.04.012

Barnett, T. P., Adam, J. C., & Lettenmaier, D. P. (2005). Potential impacts of a warming climate on water availability in snow-dominated regions. *Nature*, *438*(7066), 303–309. https://doi.org/10.1038/nature04141

Beheshti, M., Heidari, A., & Saghafian, B. (2019). Susceptibility of Hydropower Generation to Climate Change: Karun III Dam Case Study. *Water*, *11*(5), 1025.

Bivand, R. & Yu, D. (2017). spgwr: Geographically Weighted Regression. R package version 0.6-32. https://CRAN.R-project.org/package=spgwr

Blöschl, G. (1999). Scaling issues in snow hydrology. *Hydrological Processes*, *13*(14–15), 2149–2175. https://doi.org/10.1002/(SICI)1099-1085(199910)13:14/15<2149::AID-HYP847>3.0.CO;2-8

Breiman, L. E. O. (2001). Random Forests, 5–32.

Brown, R. D., & Braaten, R. O. (1998). Spatial and temporal variability of canadian monthly snow depths, 1946–1995. *Atmosphere - Ocean*, *36*(1), 37–54. https://doi.org/10.1080/07055900.1998.9649605

Brown, R. D., Brasnett, B., & Robinson, D. (2003). Gridded North American monthly snow depth and snow water equivalent for GCM evaluation. *Atmosphere - Ocean*, *41*(1), 1–14. https://doi.org/10.3137/ao.410101

Burn, D. H. (1999). Perceptions of flood risk: A case study of the Red River flood of 1997, *35*(11), 3451–3458.

Carroll, T., Cline, D., Olheiser, C., Rost, A., Nilsson, A., Fall, G., … Li, L. (2006). NOAA's National Snow Analyses. *Proceedings of the 74th Annual Meeting of the Western Snow Conference*, 1–14.

Chang, A. T. C., Foster, J. L., & Hall, D. K. (1987). Nimbus- 7 smmr derived global snow cover parameters, 39–44.

Chang, A. T. C., Foster, J. L., & Hall, D. K. (1996). Effects of forest on the snow parameters derived from mircrowave measurements during the boreas winder field campaignAIGN. *Hydrological Processes*, *10*, 1565–1574. https://doi.org/10.1002/(SICI)1099-1085(199612)10:12<1565::AID-HYP501>3.0.CO;2-5

Chang, A. T. C., Foster, J. L., Hall, D. K., Rango, A., & Hartline, B. K. (1982). Snow water equivalent estimation by microwave radiometry. *Cold Regions Science and Technology*, *5*(3), 259–267. https://doi.org/10.1016/0165-232X(82)90019-2

Chen, C., Zhao, S., Duan, Z., & Qin, Z. (2015). An Improved Spatial Downscaling Procedure for TRMM 3B43 Precipitation Product Using Geographically Weighted Regression. *IEEE Journal of Selected Topics in Applied Earth Observations and Remote Sensing*, *8*(9), 4592–4604. https://doi.org/10.1109/JSTARS.2015.2441734

Clifford, D. (2010). Global estimates of snow water equivalent from passive microwave instruments: History, challenges and future developments. *International Journal of Remote Sensing*, *31*(14), 3707–3726. https://doi.org/10.1080/01431161.2010.483482

Clow, D. W., Nanus, L., Verdin, K. L., & Schmidt, J. (2012). Evaluation of SNODAS snow depth

and snow water equivalent estimates for the Colorado Rocky Mountains, USA. *Hydrological Processes*, *26*(17), 2583–2591. https://doi.org/10.1002/hyp.9385

Cohen, Judah, & Rind, D. (1991). The effect of snow cover on climate. *Journal of Climate*, *4*(7), 689–706.

Cohen, Juval, Lemmetyinen, J., Pulliainen, J., Heinila, K., Montomoli, F., Seppanen, J., & Hallikainen, M. T. (2015). The Effect of Boreal Forest Canopy in Satellite Snow Mapping-A Multisensor Analysis. *IEEE Transactions on Geoscience and Remote Sensing*, *53*(12), 6593–6607. https://doi.org/10.1109/TGRS.2015.2444422

Comis, D. (2011). Global Warming in Western Mountains. *Agricultural Research*, *59*(1), 16–17.

Derksen, C., Walker, A., & Goodison, B. (2005). Evaluation of passive microwave snow water equivalent retrievals across the boreal forest/tundra transition of western Canada. *Remote Sensing of Environment*, *96*(3–4), 315–327. https://doi.org/10.1016/j.rse.2005.02.014

Derksen, C, & Brown, R. (2012). Spring snow cover extent reductions in the 2008 – 2012 period exceeding climate model projections. *Geophysical Research Letters*, *39*(September), 1–6. https://doi.org/10.1029/2012GL053387

Derksen, Chris. (2008). The contribution of AMSR-E 18 . 7 and 10 . 7 GHz measurements to improved boreal forest snow water equivalent retrievals, *112*, 2701–2710. https://doi.org/10.1016/j.rse.2008.01.001

Derksen, Chris, Walker, A. E., Goodison, B. E., & Strapp, J. W. (2005). Integrating In Situ and Multiscale Passive Microwave Data for Estimation of Subgrid Scale Snow Water Equivalent Distribution and Variability, *43*(5), 960–972.

Derksen, Chris, Walker, A., & Goodison, B. (2003). A comparison of 18 winter seasons of in situ and passive microwave-derived snow water equivalent estimates in Western Canada. *Remote Sensing of Environment*, *40*(1), 61–67. https://doi.org/10.1016/j.rse.2003.07.003

Dietz, A. J., Kuenzer, C., Gessner, U., & Dech, S. (2012). Remote sensing of snow – a review of available methods. *International Journal of Remote Sensing*, *33*(13), 4094–4134. https://doi.org/10.1080/01431161.2011.640964

Duan, S.-B., & Li, Z.-L. (2016). Spatial Downscaling of MODIS Land Surface Temperatures Using Geographically Weighted Regression: Case Study in Northern China. *IEEE Transactions on*

Geoscience and Remote Sensing, *54*(11), 6458–6469. https://doi.org/10.1109/TGRS.2016.2585198

Emerson, D., Vecchia, A., & Dahi, A. (2005). Evaluation of Drainage-Area Ratio Method Used to Estimate Streamflow for the Red River of the North Basin, North Dakota and Minnesota. *U.S.G.S. Scientific Investigations Report*, 5017.

Foster, J. L., Hall, D. K., Chang, A. T. C., Rango, A., Wergin, W., & Erbe, E. (1999). Effects of snow crystal shape on the scattering of passive microwave radiation. *IEEE Transactions on Geoscience and Remote Sensing*, *37*(2), 1165–1168. https://doi.org/10.1109/36.868899

Foster, James L., Sun, C., Walker, J. P., Kelly, R., Chang, A., Dong, J., & Powell, H. (2005). Quantifying the uncertainty in passive microwave snow water equivalent observations. *Remote Sensing of Environment*, *94*(2), 187–203. https://doi.org/10.1016/j.rse.2004.09.012

Foster, James L, Sun, C., Walker, J. P., Kelly, R., Chang, A., Dong, J., & Powell, H. (2005). Quantifying the uncertainty in passive microwave snow water equivalent observations. *Remote Sensing of Environment*, *94*(2), 187–203. https://doi.org/10.1016/j.rse.2004.09.012

Fotheringham, A. S., Brunsdon, C., & Charlton, M. (2002). *Geographically Weighted Reression: The Analysis of Spatially Varying Relationships*.

Friedl, M A, Mciver, D. K., Hodges, J. C. F., Zhang, X. Y., Muchoney, D., & Strahler, A. H. (2002). Global land cover mapping from MODIS : algorithms and early results, *83*, 287–302.

Friedl, Mark A, Sulla-menashe, D., Tan, B., Schneider, A., Ramankutty, N., Sibley, A., & Huang, X. (2010). Remote Sensing of Environment MODIS Collection 5 global land cover : Algorithm re fi nements and characterization of new datasets. *Remote Sensing of Environment*, *114*(1), 168–182. https://doi.org/10.1016/j.rse.2009.08.016

Gan, T. Y., Kalinga, O., & Singh, P. (2009). Comparison of snow water equivalent retrieved from SSM/I passive microwave data using artificial neural network, projection pursuit and nonlinear regressions. *Remote Sensing of Environment*, *113*(5), 919–927. https://doi.org/10.1016/j.rse.2009.01.004

Gao, Y., Xie, H., Lu, N., Yao, T., & Liang, T. (2010). Toward advanced daily cloud-free snow cover and snow water equivalent products from Terra – Aqua MODIS and Aqua AMSR-E measurements. *Journal of Hydrology*, *385*(1–4), 23–35.

https://doi.org/10.1016/j.jhydrol.2010.01.022

Gong, G. (2004). Sensitivity of atmospheric response to modeled snow anomaly characteristics. *Journal of Geophysical Research*, *109*(D6), D06107. https://doi.org/10.1029/2003JD004160

Hall, D. K., Kelly, R. E., Foster, J. L., & Chang, A. T. C. (2005). Estimation of snow extent and snow properties. *Encyclopedia of Hydrological Sciences*, *1*, 811–829. https://doi.org/10.1002/0470848944

Hancock, S., Baxter, R., Evans, J., & Huntley, B. (2013). Remote Sensing of Environment Evaluating global snow water equivalent products for testing land surface models. *Remote Sensing of Environment*, *128*, 107–117. https://doi.org/10.1016/j.rse.2012.10.004

Hedrick, A., Marshall, H. P., Winstral, A., Elder, K., Yueh, S., & Cline, D. (2015a). Independent evaluation of the SNODAS snow depth product using regional-scale lidar-derived measurements. *Cryosphere*, *9*(1), 13–23. https://doi.org/10.5194/tc-9-13-2015

Hedrick, A., Marshall, H., Winstral, A., Elder, K., Yueh, S., & Cline, D. (2015b). Independent evaluation of the SNODAS snow depth product using regional-scale lidar-derived measurements, 13–23. https://doi.org/10.5194/tc-9-13-2015

Hirsch, R. M., & Ryberg, K. R. (2012). Has the magnitude of floods across the USA changed with global CO 2 levels? *Hydrological Sciences Journal*, *57*(1), 1–9. https://doi.org/10.1080/02626667.2011.621895

Hutengs, C., & Vohland, M. (2016). Downscaling land surface temperatures at regional scales with random forest regression. *Remote Sensing of Environment*, *178*, 127–141. https://doi.org/10.1016/j.rse.2016.03.006

Immerzeel, W. W., Droogers, P., de Jong, S. M., & Bierkens, M. F. P. (2009). Large-scale monitoring of snow cover and runoff simulation in Himalayan river basins using remote sensing. *Remote Sensing of Environment*, *113*(1), 40–49. https://doi.org/10.1016/j.rse.2008.08.010

Immerzeel, W. W., Rutten, M. M., & Droogers, P. (2009). Spatial downscaling of TRMM precipitation using vegetative response on the Iberian Peninsula. *Remote Sensing of Environment*, *113*(2), 362–370. https://doi.org/10.1016/j.rse.2008.10.004

Jackson, T. J., Bindlish, R., Cosh, M. H., Zhao, T., Starks, P. J., Bosch, D. D., … Leroux, D. (2012). Validation of soil moisture and Ocean Salinity (SMOS) soil moisture over watershed networks

in the U.S. *IEEE Transactions on Geoscience and Remote Sensing*, *50*(5 PART 1), 1530–1543. https://doi.org/10.1109/TGRS.2011.2168533

Jin, Y., Ge, Y., Wang, J., Heuvelink, G. B. M., & Wang, L. (2018). Geographically weighted area-to-point regression kriging for spatial downscaling in remote sensing. *Remote Sensing*, *10*(4), 1–22. https://doi.org/10.3390/rs10040579

Josberger, E. G., Mognard, N. M., Lind, B., Matthews, R., & Carroll, T. (1998). Snowpack water-equivalent estimates from satellite and aircraft remote-sensing measurements of the Red River basin, north-central U.S.A. *Annals of Glaciology*, 119–124.

Kelly, R. E., Chang, A. T., Tsang, L., & Foster, J. L. (2003). A prototype AMSR-E global snow area and snow depth algorithm. *IEEE Transactions on Geoscience and Remote Sensing*, *41*(2 PART 1), 230–242. https://doi.org/10.1109/TGRS.2003.809118

Kim, Y., & Park, N.-W. (2017). Comparison of regression models for spatial downscaling of coarse scale satellite-based precipitation products. *International Geoscience and Remote Sensing Symposium (IGARSS)*, 1–4.

King, F., Erler, A., Frey, S., & Fletcher, C. (2020). Application of machine learning techniques for regional bias correction of SWE estimates in Ontario, Canada. *Hydrology and Earth System Sciences Discussions*, (January), 1–26. https://doi.org/10.5194/hess-2019-593

Koskinen, J., Metsa, S., Grandell, J., Ja, S., Matikainen, L., Hallikainen, M., … Hallikainen, M. (1999). Snow monitoring using radar and optical satellite data. *Remote Sensing of Environment*, *69*(1), 16–29. https://doi.org/10.1016/S0034-4257(99)00010-3

Kruopis, N., Praks, J., Arslan, A. N., Alasalmi, H., Koskinen, J., & Hallikainen, M. (1999). Passive Microwave Measurements of Snow-Covered Forest Areas in EMAC'95, *37*(5), 2699–2705.

Kunzi, K. F., & Patil, S. (1982). Snow-Cover Parameters Retrieved from Nimbus-7 Scanning Multichannel Microwave Radiometer (SMMR) Data NC-I, *75*(4), 171–180.

Kurvonen, L., & Hallikainen, M. (1997). Influence of land-cover category on brightness temperature of snow. *IEEE Transactions on Geoscience and Remote Sensing*, *35*(2), 367–377. https://doi.org/10.1109/36.563276

Kustas, W. P., Norman, J. M., Anderson, M. C., & French, A. N. (2003). Estimating subpixel surface temperatures and energy fluxes from the vegetation index – radiometric temperature

relationship, *85*, 429–440. https://doi.org/10.1016/S0034-4257(03)00036-1

Kyriakidis, P. C. (2004). A Geostatistical Framework for area to point spatial interpolation. *Geographical Analysis*, *36*(3).

Langlois, A., Royer, A., Dupont, F., Roy, A., Goita, K., & Picard, G. (2011). Improved corrections of forest effects on passive microwave satellite remote sensing of snow over boreal and subarctic regions. *IEEE Transactions on Geoscience and Remote Sensing*, *49*(10 PART 2), 3824–3837. https://doi.org/10.1109/TGRS.2011.2138145

Larue, F., Royer, A., De Sève, D., Langlois, A., Roy, A., & Brucker, L. (2017). Validation of GlobSnow-2 snow water equivalent over Eastern Canada. *Remote Sensing of Environment*, *194*, 264–277. https://doi.org/10.1016/j.rse.2017.03.027

Li, Q., & Kelly, R. E. J. (2017). Correcting Satellite Passive Microwave Brightness Temperatures in Forested Landscapes Using Satellite Visible Reflectance Estimates of Forest Transmissivity. *IEEE Journal of Selected Topics in Applied Earth Observations and Remote Sensing*, *10*(9), 3874–3883. https://doi.org/10.1109/JSTARS.2017.2707545

Liaw, A., & Wiener, M. (2002). Classification and Regression by randomForest. *R News*, *2*(December), 18–22.

Liu, J., Li, Z., Huang, L., & Tian, B. (2014). Hemispheric-scale comparison of monthly passive microwave snow water equivalent products. *Journal of Applied Remote Sensing*, *8*(1), 084688. https://doi.org/10.1117/1.jrs.8.084688

Loveland, T. R., & Belward, A. S. (1997). The IGBP-DIS global 1km land cover data set , DISCover : First results, *1161*. https://doi.org/10.1080/014311697217099

Luojus, K., Pulliainen, J., Takala, M., Lemmettyinen, J., Kangwa, M., Eskelinen, M., … Foppa, N. (2014). GlobSnow-2 Final Report, (1).

Matsui, T., Lakshmi, V., & Small, E. (2003). Links between snow cover, surface skin temperature, and rainfall variability in the North American monsoon system. *Journal of Climate*, *16*(11), 1821–1829. https://doi.org/10.1175/1520-0442(2003)016<1821:LBSCSS>2.0.CO;2

Mätzler, C., & Standley, A. (2000). Technical note: Relief effects for passive microwave remote sensing. *International Journal of Remote Sensing*, *21*(12), 2403–2412. https://doi.org/10.1080/01431160050030538

Menne, M. J., Durre, I., Vose, R. S., Gleason, B. E., & Houston, T. G. (2012). An Overview of the Global Historical Climatology Network-Daily Database. *Journal of Atmospheric and Oceanic Technology*, *29*, 897–910. https://doi.org/10.1175/JTECH-D-11-00103.1

Mudryk, L. R., Derksen, C., Kushner, P. J., & Brown, R. (2015). Characterization of Northern Hemisphere snow water equivalent datasets, 1981–2010. https://doi.org/10.1175/JCLI-D-15-0229.1

Neumann, N. N., Derksen, C., Smith, C., & Goodison, B. (2006). Characterizing local scale snow cover using point measurements during the winter season. *Atmosphere - Ocean*, *5900*. https://doi.org/10.3137/ao.440304

Pardo-Igúzquiza, E., & Atkinson, P. M. (2007). Modelling the semivariograms and cross-semivariograms required in downscaling cokriging by numerical convolution-deconvolution. *Computers and Geosciences*, *33*(10), 1273–1284. https://doi.org/10.1016/j.cageo.2007.05.004

Pulliainen, J. (2006). Mapping of snow water equivalent and snow depth in boreal and sub-arctic zones by assimilating space-borne microwave radiometer data and ground-based observations. *Remote Sensing of Environment*, *101*(2), 257–269. https://doi.org/10.1016/j.rse.2006.01.002

R Core Team (2018). R: A language and environment for statistical computing. R Foundation for Statistical Computing, Vienna, Austria. URL https://www.R-project.org/.

Räisänen, J. (2008). Warmer climate: Less or more snow? *Climate Dynamics*, *30*(2–3), 307–319. https://doi.org/10.1007/s00382-007-0289-y

Rannie, W. (2016). The 1997 flood event in the Red River basin: Causes, assessment and damages. *Canadian Water Resources Journal*, *41*(1–2), 45–55. https://doi.org/10.1080/07011784.2015.1004198

Rice, J. S., Emanuel, R. E., Vose, J. M., & Nelson, S. A. C. (2015). Continental U.S. streamflow trends from 1940 to 2009 and their relationships with watershed spatial characteristics. *Water Resources Research*, *51*, 6262–6275. https://doi.org/10.1002/2014WR016367.Received

Robinson, P. J. (1997). Climate change and hydropower generation. *International Journal of Climatology*, *17*(9), 983–996. https://doi.org/10.1002/(sici)1097-0088(199707)17:9<983::aid-joc174>3.3.co;2-9

Ryan, Thomas P. (2009). *Modern Regression Methods (2nd Edition) - 1. Introduction.* John Wiley &

Sons.

Schwert, D. P. (2003). A Geologist's Perspective on the Red River of the North: History, Geography, and Planning / Management Issues. *Proceedings 1st International Water Conference*, 1–16.

Sexstone, G. A., & Fassnacht, S. R. (2014). What drives basin scale spatial variability of snowpack properties in northern Colorado? *Cryosphere*, *8*(2), 329–344. https://doi.org/10.5194/tc-8-329-2014

Singh, P. R., & Gan, T. Y. (2000). Retrieval of Snow Water Equivalent Using Passive Microwave Brightness Temperature Data. *Remote Sensing of Environment*, *74*.

Snauffer, A. M., Hsieh, W. W., & Cannon, A. J. (2016). Comparison of gridded snow water equivalent products with in situ measurements in British Columbia, Canada. *Journal of Hydrology*, *541*, 714–726. https://doi.org/10.1016/j.jhydrol.2016.07.027

Stewart, I., Cayan, D., & Dettinger, M. (2004). Changes in snowmelt runoff timing in western North America under a "business as usual" climate change scenario. *Climatic Change*, *62*, 217–232.

Stoner, J. D., Lorenz, D. L., Wiche, G. J., & Goldstein, R. M. (1993). Red River of the North Basin, Minnesota, North Dakota, and South Dakota. *JAWRA Journal of the American Water Resources Association*, *29*(4), 575–615. https://doi.org/10.1111/j.1752-1688.1993.tb03229.x

Sturm, M., Holmgren, J., & Liston, G. E. (1995). A seasonal snow cover classification system for local to global applications. *Journal of Climate*, *8*(5), 1261–1283. https://doi.org/10.1175/1520-0442(1995)008<1261:ASSCCS>2.0.CO;2

Sturm, Matthew, Goldstein, M. A., & Parr, C. (2017). Water and life from snow: A trillion dollar science question. *Water Resources Research*, (53), 3534–3544. https://doi.org/10.1002/2017WR020840.Received

Sturm, Matthew, Taras, B., Liston, G. E., Derksen, C., Jonas, T., & Lea, J. (2010). Estimating Snow Water Equivalent Using Snow Depth Data and Climate Classes. *Journal of Hydrometeorology*, *11*(6), 1380–1394. https://doi.org/10.1175/2010jhm1202.1

Takala, M., Luojus, K., Pulliainen, J., Derksen, C., Lemmetyinen, J., Kärnä, J. P., … Bojkov, B. (2011). Estimating northern hemisphere snow water equivalent for climate research through assimilation of space-borne radiometer data and ground-based measurements. *Remote Sensing of Environment*, *115*(12), 3517–3529. https://doi.org/10.1016/j.rse.2011.08.014

Tedesco, M., & Narvekar, P. S. (2010). Assessment of the NASA AMSR-E SWE Product. *IEEE Journal of Selected Topics in Applied Earth Observations and Remote Sensing*, *3*(1), 141–159. https://doi.org/10.1109/JSTARS.2010.2040462

Teng, H., Shi, Z., Ma, Z., & Li, Y. (2014). Estimating spatially downscaled rainfall by regression kriging using TRMM precipitation and elevation in Zhejiang Province , southeast China. *International Journal of Remote Sensing*, *35*(22), 7775–7794. https://doi.org/10.1080/01431161.2014.976888

Todhunter, P. E. (2016). Mean hydroclimatic and hydrological conditions during two climatic modes in the Devils Lake Basin, North Dakota (USA). *Lakes and Reservoirs: Research and Management*, *21*(4), 338–350. https://doi.org/10.1111/lre.12152

Vecchia, A. V. (2008). Climate simulation and flood risk analysis for 2008–40 for Devils Lake, North Dakota. *U.S. Geological Survey Scientific Investigations Report 2008–5011*, 28. Retrieved from http://pubs.usgs.gov/sir/2008/5011/pdf/sir2008-5011web.pdf

Vuyovich, C. M., Jacobs, J. M., & Daly, S. F. (2014). Comparison of passive microwave and modeled estimates of total watershed SWE in the continental United States. *Water Resources Research*, *50*, 2–2. https://doi.org/10.1111/j.1752-1688.1969.tb04897.x

Wang, Q., Shi, W., & Atkinson, P. M. (2016). Area-to-point regression kriging for pan-sharpening. *ISPRS Journal of Photogrammetry and Remote Sensing*, *114*, 151–165. https://doi.org/10.1016/j.isprsjprs.2016.02.006

Wang, Q., Shi, W., Atkinson, P. M., & Zhao, Y. (2015). Downscaling MODIS images with area-to-point regression kriging. *Remote Sensing of Environment*, *166*, 191–204. https://doi.org/10.1016/j.rse.2015.06.003

Wang, Shuguo, Li, X., Ge, Y., Jin, R., Ma, M., Liu, Q., … Liu, S. (2016). Validation of regional-scale remote sensing products in china: From site to network. *Remote Sensing*, *8*(12), 1–26. https://doi.org/10.3390/rs8120980

Wang, Shusen, & Russell, H. A. J. (2016). Forecasting Snowmelt-Induced Flooding Using GRACE Satellite Data: A Case Study for the Red River Watershed. *Canadian Journal of Remote Sensing*, *42*(3), 203–213. https://doi.org/10.1080/07038992.2016.1171134

Wheeler, D. C., & Páez, A. (2010). Geographically Weighted Regression. *Handbook of Applied*

Spatial Analysis, 461–486. https://doi.org/10.1007/978-3-642-03647-7

Wrzesien, M. L., Durand, M. T., Pavelsky, T. M., Howat, I. M., Margulis, S. A., & Huning, L. S. (2017). Comparison of Methods to Estimate Snow Water Equivalent at the Mountain Range Scale : A Case Study of the California Sierra Nevada. https://doi.org/10.1175/JHM-D-16-0246.1

Yu, G. (Eugene), Di, L., & Yang, W. (2008). DOWNSCALING OF GLOBAL SOIL MOISTURE USING AUXILIARY DATA Genong (Eugene) Yu, Liping Di, and Wenli Yang Center for Spatial Information Science and Systems, George Mason University, 6301 Ivy Ln, Suite #620, Greenbelt, MD 20770, USA. *2008 IEEE International Geoscience and Remote Sensing Symposium – Proceedings*, *3*, III230–III233.

Yueh, S., Dinardo, S., Akgiray, A., West, R., Cline, D., & Elder, K. (2009). Airborne Ku-band radar remote sensing of terrestrial snow cover. *IEEE Transactions on Geoscience and Remote Sensing*, *47*(10), 3347–3364. https://doi.org/10.1109/IGARSS.2007.4423023

Zaksek, K., & Ostir, K. (2012). Remote Sensing of Environment Downscaling land surface temperature for urban heat island diurnal cycle analysis. *Remote Sensing of Environment*, *117*, 114–124. https://doi.org/10.1016/j.rse.2011.05.027

Zhang, T. (2005). Influence of the seasonal snow cover on the ground thermal regime: An overview. *Reviews of Geophysics*, *43*(4). https://doi.org/10.1029/2004RG000157.1.INTRODUCTION

Zhang, X., Li, H. Y., Deng, Z. D., Ringler, C., Gao, Y., Hejazi, M. I., & Leung, L. R. (2018). Impacts of climate change, policy and Water-Energy-Food nexus on hydropower development. *Renewable Energy*, *116*, 827–834. https://doi.org/10.1016/j.renene.2017.10.030

Zheng, H., Barta, D., & Zhang, X. (2014). Lesson learned from adaptation response to Devils Lake flooding in North Dakota, USA. *Regional Environmental Change*, *14*(1), 185–194. https://doi.org/10.1007/s10113-013-0474-y